CHALMERS

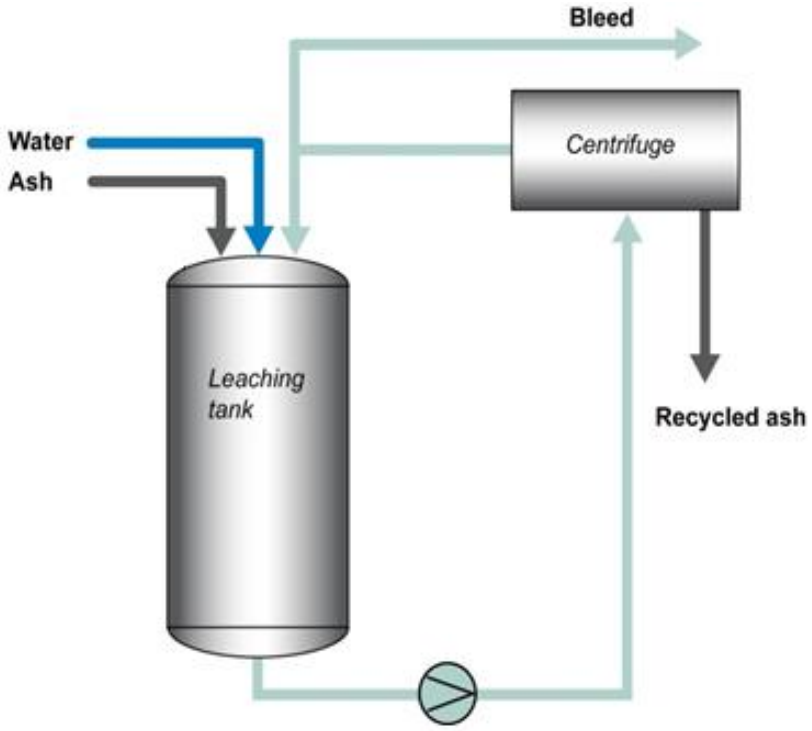

Calculation tool for the treatment of electrostatic precipitator ash in Metso's ash leaching process

Master's Thesis within the Innovative and Sustainable Chemical Engineering programme

MALIN LARSSON

Department of Chemical and Biological Engineering

Forest Products and Chemical Engineering

CHALMERS UNIVERSITY OF TECHNOLOGY

Gothenburg, Sweden 2012

MASTER'S THESIS

Calculation tool for the treatment of electrostatic precipitator ash in Metso's ash leaching process

Master's Thesis within the Innovative and Sustainable Chemical Engineering programme

MALIN LARSSON

SUPERVISORS:

Kai Lüder

Martin Wimby

Therese Hedlund

EXAMINER

Hans Theliander

Department of Chemical and Biological Engineering

Forest Products and Chemical Engineering

CHALMERS UNIVERSITY OF TECHNOLOGY

Gothenburg, Sweden 2012

Calculation tool for the treatment of electrostatic precipitator ash in Metso's ash leaching process
Master's Thesis within the Innovative and Sustainable Chemical Engineering programme

MALIN LARSSON

Department of Chemical and Biological Engineering

Forest Products and Chemical Engineering

Chalmers University of Technology

SE-412 96 Göteborg

Sweden

Telephone: + 46 (0)31-772 1000

Cover:

Simplified process flow diagram of an ash leaching process.

Chalmers Reproservice

Gothenburg, Sweden 2012

Calculation tool for the treatment of electrostatic precipitator ash in Metso's ash leaching process

Master's Thesis in the Innovative and Sustainable Chemical Engineering programme

MALIN LARSSON

Department of Chemical and Biological Engineering

Forest Products and Chemical Engineering

Chalmers University of Technology

ABSTRACT

Two different solubility models have been developed for Metso's Ash Leach process. The backbone of the models consists of mass balances describing the overall process and the individual components; leaching tank and centrifuge. The difference between the models is the modeling of the dissolution of the components included in the electrostatic precipitator ash in water. Electrostatic precipitator ash is mainly composed of five components; Na^+, K^+, Cl^-, SO_4^{2-} and CO_3^{2-}, which in solid phase leads to formation of the salts Na_2SO_4, Na_2CO_3, NaCl, K_2SO_4, K_2CO_3 and KCl. The main components in the ash are normally sodium and sulphate, but ashes consisting of high amounts of carbonate may also occur. The first model, Model I, is a simple model based solely on mass balances and a fixed amount of ash dissolved in a saturated solution. Na_2SO_4 is the only salt predicted to be present in the solid phase. All other salts are assumed to be completely dissolved.

For the other model, regressions of literature data and experimental data from units in operation have been used. The dissolution predicted by Model II is dependent on the system Na_2SO_2-K_2SO_4-Na_2CO_3 and its dependence on temperature. This system was used in order to investigate the possibility to use a four component system when describing the solubility of a five component system. NaCl, KCl and K_2CO_3 are assumed to be completely dissolved.

It is also important to consider the total amount of ash dissolved in a saturated solution. The amount of dissolved ash in water is commonly considered to be between 29-33 wt% in a saturated solution for units in operation. Three different amounts of ash in water have been investigated: One regression is depending on the K/(K+Na) molar ratio in the slurry, and two fixed amounts of ash at 31 wt% and 32 wt% dissolved solids in the liquid phase. The predicted results using these settings are compared with the predicted results using the amount of dissolved ash specified in the experimental data.

Finally, the efficiencies predicted by Models I and II are compared to simulations performed by Chemcad including corrections done by Metso Power.

Both Models I and II predict the reject composition well for slurries containing low contents of carbonate and potassium at an ash to water ratio in slurry of 800 g ash/ l water, if no recirculation is used. When the ash to water ratio increases, both Model I and II predicts the concentration of negatively charged ions well for a slurry containing a low amount carbonate. But the concentration potassium and sodium are predicted to be higher respectively lower than the experimental data.

When recirculation is used, the predicted reject composition deviates from the experimental data. For Mill 1, this probably depends on the fact that suspended solids are carried over to the liquid phase. In reality suspended solids may be carried over to the liquid phase if the centrifuge is not working properly. However, the recycled ash composition conforms well to the experimental data for Mill 1, but for Mill 2 larger deviations occur due to the higher amounts of carbonate in the slurry and a lower dryness of the recycled ash. The same result occurs when comparing efficiencies. For Mill 1 the predicted efficiencies of both Models I and II conform relatively well to the efficiencies based on experimental data and the efficiencies predicted by Chemcad. Only smaller deviations occur. For Mill 2 deviations occur from experimental data for all models including Chemcad. Model II produces the best prediction of carbonate and sulphate efficiencies whereas Chemcad and Model I predict significantly higher recovery efficiency than what is the case in reality.

It is concluded that all models provides good estimations of the reject composition for ashes containing low carbonate and potassium contents when no liquid is recycled back to the leaching tank. But when the carbonate content increases the deviations increase as well. In order to find correlations for systems including larger amounts of potassium and carbonate a larger quantity and more accurate data are needed. It may be necessary to develop a thermodynamic model in order to produce more accurate predictions about such a system. When the recirculation ratio is increased an increased concentration potassium and carbonate will be present in the liquid phase, which makes it important to have a model that provides accurate predictions of the precipitation of burkeite and glaserite.

When modeling different specified amounts of ash that are dissolved in a saturated solution, deviations occur when the results are compared with the predicted values using the specified amount of ash dissolved in the reject. This indicates that an accurate amount of ash dissolved in a saturated solution is needed to obtain accurate compositions in the liquid phase.

Key words:

Leaching, Chemical recovery, Non-process elements, Solubility, Electrostatic precipitator ash, Chloride, Potassium, Sodium sulphate

Contents

Preface

This report is a Master's Thesis project for the degree of Master of Science in Chemical Engineering at Chalmers University of Technology. The project has been performed at Metso Power in Gothenburg in collaboration with the Department of Forest Products and Chemical Engineering at Chalmers University of Technology during the spring and summer of 2012. The supervisors were Kai Lüder, Martin Wimby and Therese Hedlund at Metso Power. The examiner at Chalmers University of Technology was Hans Theliander.

First of all, I would especially like to thank my supervisors Kai Lüder, Martin Wimby and Therese Hedlund for their commitment and assistance provided throughout the entire project. Major effort has been put into discussions and commenting on the report.

I would also like to show my appreciation to all employees at Metso Power for their warm welcoming and support, whenever I have had questions.

Lastly, I would like to thank my family and friends for being interested in my work and for supporting me through setbacks. A special thanks to Simon who is always there for me and have supported and encouraged me during the project.

Malin Larsson
Gothenburg, 2012

Notations

Roman letters

a	Activity
ΔG	Difference in Gibbs free energy
ΔH	Enthalpy change
$\dot{m}$	Mass flow
n	Number of molecules
P	Total pressure
R	Molar gas constant
ΔS	Entropy change
T	Absolute temperatur
x_i	Molar fraction in liquid

Greek letters

γ_i	Activity coefficient
μ_i	Chemical potential
μ_i°	Standard chemical potential

Subscripts

ash, in	Electrostatic precipitator ash to leaching
aq	Aqueous solution
$bleed$	Purged liquid stream
H_2O	Water to leaching
i	Any specie
$reject$	Liquid stream rich in chloride and potassium
$slurry$	Suspended solids together with diluted solids before separation
$recirc$	Recycled reject

Abbreviations

BLS	Black liquor solids
Cl^-	Chloride
CO_3^{2-}	Carbonate
DS	Dry solids
ds	Dissolved solids
$dust$	Electrostatic precipitator ash
ESP	Electrostatic precipitator
K^+	Potassium

KCl	Potassium chloride
K_2CO_3	Potassium carbonate
K_2SO_4	Potassium sulphate
Na^+	Sodium
$NaCl$	Sodium chloride
Na_2CO_3	Sodium carbonate
Na_2S	Sodium sulphide
Na_2SO_4	Sodium sulphate
RBD	Recovery Boiler Design
SO_4^{2-}	Sulphate
ss	Suspended solids

1 Introduction

In pulp and paper industry there is a continuously ongoing work for closing processes where the main focus is to save energy and chemicals (1). Saving energy and chemicals reduces the environmental impact and cost of make-up chemicals. One way to reduce the usage of chemicals is to remove non-process elements, such as chlorides and potassium, from the electrostatic precipitator ash. The electrostatic precipitator ash from the recovery boiler contains five main components which result in different ionic alkali salts, for example Na_2SO_4, Na_2CO_3, NaCl, K_2SO_4, K_2CO_3 and KCl (2). Since chlorides and potassium cause corrosion and plugging in the recovery boiler they need to be separated from the process flow. Traditionally a part of the ash flow has been dumped to avoid this problem. But since dumping also means losing valuable Na_2SO_4, different processes for separating chlorides and potassium from the process flow have been developed. One of these is the leaching process, where precipitator ash is leached with water (1).

In an ash leaching process the difference in water solubility of salts occurring in the precipitator ash is used in order to separate chloride and potassium from sulphate. This separation leads to enhanced Na_2SO_4 recovery and removal of non-process elements such as chlorides and potassium (3). The interaction between ions and the solubility of different salts are therefore important parameters when modeling the leaching process. For dimensioning of ash leaching plants today, Metso Power uses Chemcad to solve the component and mass balances. The Pitzer electrolyte model available in Chemcad is applied to predict the solubility of precipitator ash. The calculation procedure in Chemcad comprises several steps which are not discussed in this report. The results are exported from Chemcad to Excel where important corrections must be made in the results due to errors originating from weaknesses in the Chemcad model. Other issues with using Chemcad for this purpose are that Metso Power has a limited number of licenses for Chemcad and the program is therefore not accessible to everyone. In some situations the steady state calculations for the ash leaching system has difficulties to converge, which seems to be a problem with new versions of the software. New versions might also produce altered results when comparing with previous versions. Since Excel is already used for corrections and processing of data, it would have been preferable to use this software throughout the entire procedure.

In literature a limited number of models predicting the solubility of precipitator ash have been found. Two models for the prediction of the solubility of precipitator ash have been published by Saturnino (4, 5). Saturnino has modeled this dissolution in the OLI software (5) but also developed a regression model (4). The aqueous model in the OLI electrolyte simulation software is an electrolyte thermodynamic model based on published experimental data. The model uses data regression wherever possible and produce estimations and extrapolations where required (6). According to Saturnino, the estimated solubilities of the ash conform well with experimental data, but to somewhat lower predicted concentration of Cl^- and higher predicted concentration of Na^+ (5). The regression model developed by Saturnino is based on experimental data. The model equation consists of a third degree polynomial which depends on temperature, alkalinity (hydroxide plus sulphide concentration in grams per litre), molar ratio of potassium over potassium and sodium in the ash and compound parameters. The curves provide the solubility of the negatively charged ions (Cl^-, CO_3^{2-} and SO_4^{2-}) provided that the solution is in equilibrium with the positively charged ions (K^+, Na^+). The data cover a temperature range from 50 to 100 °C (7). Predictions compared to the experimental work performed by Jaretun (8) give similar results for the extraction of the elements.

1.1 Purpose

The primary aim with the Master's Thesis project is to develop a calculation tool for solubilities in Excel for Metso's Ash Leach Process in order to become more or less independent on Chemcad. An Excel data sheet fitted with relevant equations to describe the equilibrium solubility of the different ions when the ash is dissolved, should be developed and evaluated. The ambition is to implement and evaluate an accurate model for the predictions of aqueous solubilities at equilibrium in the mass balance calculation. It is important to keep the model as simple as possible in order to make it easy to follow and maintain. The major advantage with an in-house software is that such a calculation tool is available to all Metso engineers. If one wish to change the chemical model inside the calculation tool in the future it can be easily done, which is not the case for a commercial program such as Chemcad.

1.2 Scope

This paragraph describes the limitations of the project.

- The objective is to develop a model for a single step ash leaching process.
- The components included in the models are Na^+, K^+, Cl^-, SO_4^{2-} and CO_3^{2-} forming the salts NaCl, KCl, Na_2SO_4, K_2SO_4, Na_2CO_3 and K_2CO_3.
- The operating temperature of the ash leaching process is normally in the range of 70-90 °C. The models are based on experimental data in this range and are therefore only valid in this temperature interval.
- Separation in the centrifuge is assumed to be total, which means that no solids are discharged with the reject, i.e. the liquid phase.
- The fact that different ash composition affects the dryness of the outgoing ash is not considered in the project.
- Dynamic effects, for example time required to reach equilibrium between solid and liquid phase, is not considered in this report. The residence time in the leaching tankt is long enough for the system to reach steady state. This assumption is consistent with the experimental data performed by Jaretun (8).

2 Background

A brief background to the Kraft pulping process is provided in this chapter. The setup of the ash leaching process together with the section about solubilities provides the background to the developed models.

2.1 Kraft Pulping

The ash leaching principle can be used in the Kraft pulping process, which is the most common way of manufacturing pulp in Sweden. The Kraft process can handle almost all species of softwood and hardwood, provides strong pulp and is economically feasible due to high chemical recovery efficiency, about 97% (9). It is an effective technology that provides recycling of pulping chemicals and generation of steam and electrical power when black liquor is burnt (9). Sodium hydroxide and sodium sulphide are used as active cooking chemicals, which removes lignin and hemicelluloses from cellulose. About fifty percent of the ingoing wood is dissolved in the process together with the spent pulping chemicals, resulting in a stream called weak black liquor, as can be seen in Figure 1. The weak black liquor is separated from the pulp and evaporated in order to increase the concentration before entering the recovery boiler as heavy black liquor. When the black liquor is burnt, a smelt bed mainly consisting of Na_2CO_3 and Na_2S are formed in the lower part of the furnace (10). The flue gas contains mainly of Na_2SO_4 but also other inorganic compounds such as cadmium, chlorides and potassium which accumulate in the electrostatic precipitator (ESP) forming ESP ash.

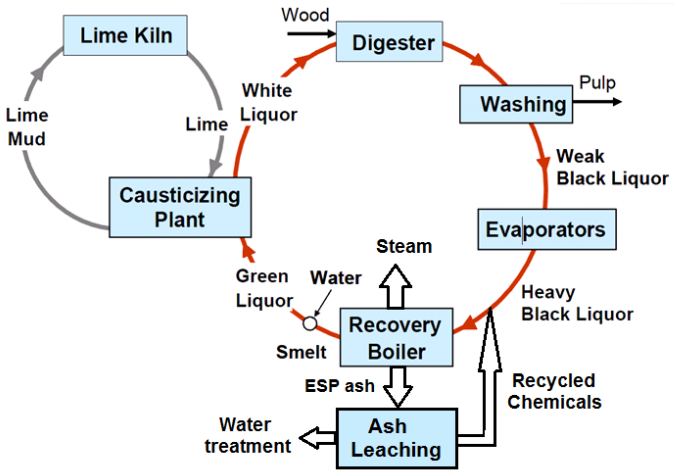

Figure 1. The kraft chemical recovery cycle including the ash leaching process (9).

Since the ESP ash contains a large fraction Na_2SO_4, which is a valuable make-up chemical, it is favourable to recycle it back to the process. The main part of the chlorides and potassium accumulate in the ESP ash, and therefore this ash is treated in the ash leaching process. As mentioned in Chapter 1, the ash leaching system utilises the differences in solubility of different compounds in order to separate them from each other. The process is built on the fact that NaCl and KCl are more soluble in water than Na_2SO_4. This means that large fractions of NaCl and KCl normally can be removed and disposed for water treatment, where Na_2SO_4 is recycled back to the recovery cycle.

2.2 Recovery Boiler

The recovery boiler is one of the most important equipments in pulp mills since it recycles cooking chemicals and produces energy. The chemical, physical and combustion properties vary among mills depending on location, wood species, pulp yield, white liquor properties and ratio between wood and chemicals among other factors (9).

Concentrated black liquor from the evaporation plant is sprayed into the recovery boiler and burnt in deficit of oxygen leading to the reduction of Na_2SO_4 to Na_2S. The inorganic sulphur and sodium can be recovered as a molten ash smelt containing mostly Na_2S and Na_2CO_3. The smelt is dissolved in water, forming green liquor, before it is sent to the causticizing plant where Na_2CO_3 is converted to NaOH. A fraction of the burnt black liquor in the recovery boiler will vaporize from the char bed, follow the flue gases, and accumulate in the ESP as ESP ash (6).

2.2.1 ESP ash composition

The ESP ash consists of inorganic compounds which usually enter the mill with the wood and to a smaller extent with the make-up chemicals and water (11). The amount of inorganic non-process elements entering the mill depends on wood type, location of the mill and transportation route. ESP ash compositions from three mills are presented in Table 1. These mills will be referred to as Mill 1, Mill 2 and Mill 3. The ash from Mill 1 is a low carbonate ash, whereas Mill 2 and Mill 3 produce ash with relatively high carbonate content. The chloride content is similar for all mills and the potassium content is somewhat lower for Mill 2 and higher for Mill 3.

Table 1. Average ESP ash composition from three different mills; Mill 1, Mill 2 and Mill 3. The composition for each analysis in ash, reject, slurry and recycled ash is presented in Appendix C.

Average ash composition (wt% dry ash)	*Mill 1*	*Mill 2*	*Mill 3*
Cl^-	3,64%	3,79%	4,38%
K^+	4,37%	2,97%	5,19%
Na^+	29,68%	34,07%	34,21%
$SO4^{2-}$	62,08%	41,64%	30,12%
$CO3^{2-}$	0,23%	17,52%	26,10%
Na_2SO_4	84,48%	58,57%	40,89%
Na_2CO_3	0,38%	29,44%	42,32%
NaCl	5,52%	5,95%	6,63%
K_2SO_4	8,96%	3,69%	4,48%
K_2CO_3	0,04%	1,96%	4,92%
KCl	0,61%	0,39%	0,75%
Average ratio of ash to water in slurry (g ash/l H_2O)	1200	800	900
Temperature (ºC)	90	90	90

Chloride, potassium, cadmium, calcium and arsenic are examples of undesirable non-process elements. Chlorides and potassium accumulate in the pulping liquors and have higher solubility than for example cadmium (12). These non process elements accumulate until they reach a steady-state concentration dependent on inputs, degree of mill closure and liquor sulphidity. When mills close up, which means that they decrease the dumping of cooking chemicals, the input of chloride and potassium becomes increasingly important. An increased closure can accumulate chloride and potassium up to 4-12 times greater than mills which operate fairly open (13).

As mentioned earlier the chlorides and potassium accumulate in the black liquor, which is burnt in the recovery boiler. KCl and NaCl have a higher vapor pressure than Na_2S and will therefore volatilize from the char bed in the recovery boiler and accumulate in the ESP ash (3). This means that the bed temperature in the recovery boiler has a significant effect on the enrichment of chlorides and potassium in the ESP ash. The ESP ash is mainly composed of five different ions; sodium, sulphate, potassium, chloride and carbonate which mainly form Na_2SO_4, NaCl, Na_2CO_3, K_2SO_4, KCl and K_2CO_3. The melting point of the ESP ash is influenced by the potassium and chloride concentrations in the fired black liquor (11). An increase in potassium or chloride concentrations result in a lower melting point of the ash, leading to increased deposits and plugging in the upper furnace sections which lead to the fact that consecutive downtime is required for washing the boiler with water. The downtime needs to be minimized since it results in economical losses. Deposits are sticky when 15-70% of the ash is in the molten state. The temperature when 15% of the ash particles have melted is called the sticky temperature, which is denoted $T_{15.}$ The temperature when 70% is in molten state is called the radical deformation temperature, denoted T_{70}. Figure 2 shows the effect of chloride on T_{15} and T_{70} for a typical carry over deposit containing 5 mole% $K^+/(K^+ + Na^+)$ (13). An increase in chloride content lowers both the sticky and the radical deformation temperature. The effect of potassium is similar to chloride, but not as prominent (13, 14). At a low chloride concentration, potassium gives only a small effect on the sticky temperature, illustrated in the picture to the right in Figure 2. But when the chloride concentration increases, potassium has an increased effect on lowering the sticky temperature.

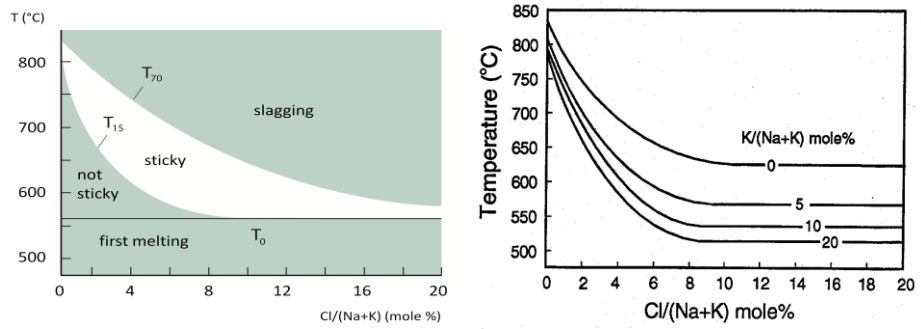

Figure 2. To the left, the sticky temperature is shown as a function of the molar ratio between chloride divided by sodium and potassium for a typical carry over deposit containing 5 mole% $K^+/(K^+ + Na^+)$ (13, 15). The sticky temperature dependence of potassium in the ash is shown in the right picture as a function of the molar ratio $Cl^-/(Na^+ + K^+)$ (13). The plots are regressions of experimental data.

When particles stick to the walls and tubes of the recovery boiler it leads to lower heat transfer through the surface and reduced temperature of the generated steam. The region of sticky ash for high and low concentration of chlorides and potassium can be seen in Figure 3. High potassium and chloride concentrations result in deposits in the upper part of the boiler, shown as the marked region in the left picture in Figure 3, where the temperatures of the flue gases are lower. In this region the deposits have a tendency to harden and are difficult to remove with sootblowers which leads to a increased risk of plugging (16).When the concentration of chlorides and potassium are lower, the fouling occurs in the region marked in the right picture of Figure 3. In this region the deposits are easier to remove with sootblowing and the downtime for washing decreases.

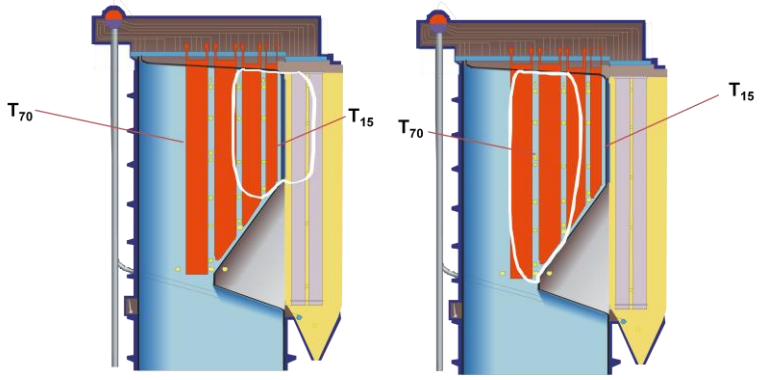

Figure 3. The left picture shows the deposit area with a high concentration of chlorides and potassium. To the right the deposit area for a low concentration chloride and potassium is shown (15).

Removal of potassium and chloride from the ESP ash is a very important issue in future chemical recovery cycles, where the focus is to reduce the amount of chemicals used in the process. Ash leaching of ESP ash is one way of decreasing the content of these two non-process elements (3). This is because of the enrichment in the ash, but also since the ash is easier to handle in comparison to liquors. The purge of chloride and potassium becomes more and more important due to the construction of new recovery boilers operating at higher temperatures and steam pressures.

2.3 Ash leaching principle and process

The purpose of the ash leaching system is to decrease the concentration of chlorides and potassium in the liquor cycle while Na_2SO_4 is recovered. Alternative ash treatment systems available are ion exchange, evaporation/crystallisation and freeze crystallisation (3). These are all interesting processes but will not be further discussed here.

The usage of an ash leaching plant reduces the environmental impact and cost for make-up chemicals compared to purging of ESP ash. The ash leaching system keeps the major part of the heavy metals, such as cadmium, in the solids that are brought back to the liquor cycle. The heavy metals can then be separated elsewhere, for instance in filtering of the green liquor dregs. The amount of ESP ash to be treated in the leaching plant in order to maintain the right chemical balance depends on the input of potassium and chlorides to the mill. The leaching step is selective, meaning that most of the potassium and chlorides are dissolved in the liquid phase while a large fraction of Na_2SO_4 remains solid and can be separated from the liquid phase and returned to the liquor cycle. The dissolution principle of NaCl, KCl and Na_2SO_4 is by a simplified picture shown in Figure 4. Initially the ash is mixed with water to form a suspension. When equilibrium is obtained between the liquid and solid, almost all NaCl and KCl are dissolved while Na_2SO_4 stays in solid phase. The last unit operation is separation of the liquid containing the dissolved salts from the solid fraction.

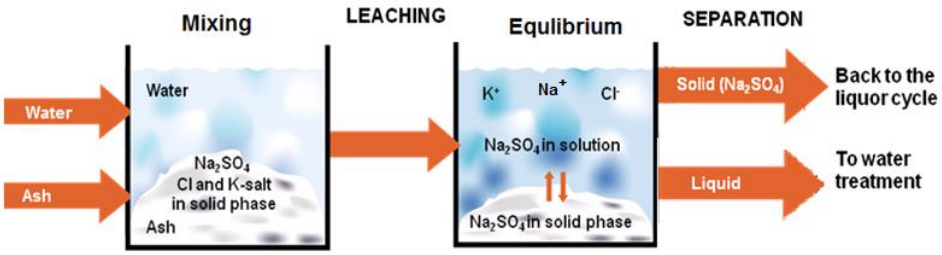

Figure 4. A simplified picture of the ash leaching principle (15). In reality, Na_2SO_4 is not the only component in the solid phase.

In Figure 5 a simplified process flow diagram is shown for the ash leaching process. The ash is mixed with warm water in an agitated leaching tank which results in the formation of a slurry. The slurry is a partly diluted mixture which contains suspended solids and diluted solids in water. This initial step corresponds to the mixing and equilibrium step shown in Figure 4. Most of the chlorides and potassium dissolve in the water while the main part of Na_2SO_4 remains solid.

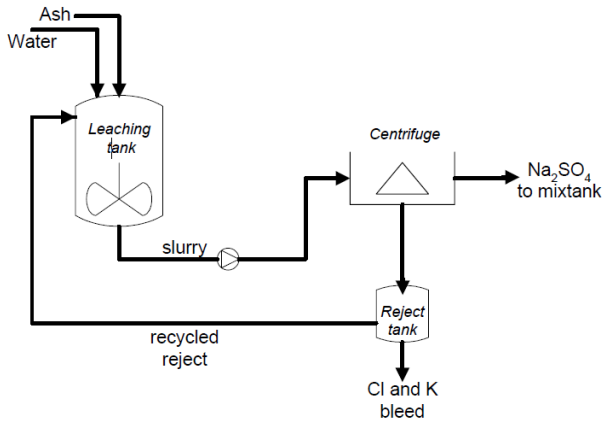

Figure 5. Simplified process flow diagram of an ash leaching process (10).

The slurry is transferred from the leaching tank to a centrifuge where liquid and solids are mechanically separated by centrifugal forces. The fraction dissolved solids and suspended solids in slurry, reject and recycled ash are principally shown in Figure 6. In an ideal separation step the separation between suspended solids and reject is total, which means that no suspended solids are present in the reject.

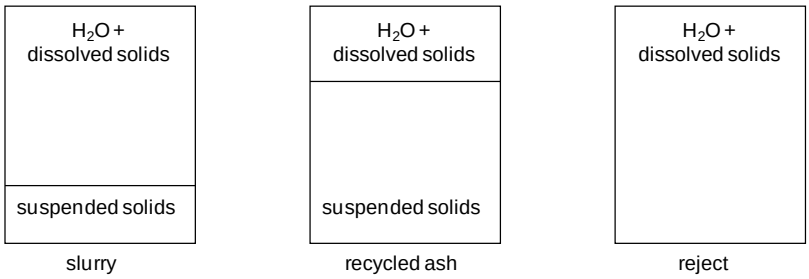

Figure 6. Dissolved and suspended solids in the process streams entering and exiting the centrifuge.

In reality this separation depends on the centrifugal force, which include the density difference between solid and liquid phase, viscosity, particle size and mechanical work of the centrifuge. A smaller particle size makes it more difficult to dewater the recycled ash which results in a decreased dryness. When the dewatering decreases a larger fraction of reject will be present in the recycled solids, which leads to a decreased efficiency. The normal dryness of the recycled solids is 70-90% depending mainly on carbonate content and type of centrifuge. The dryness of the treated ash should not be below 80 % to guarantee an efficient separation step. If smaller particles are present, it will also increase the risk that particles are carried over to the liquid phase which results in suspended solids in the reject.

The recycled ash containing Na_2SO_4 is mixed with virgin black liquor in the mix tank and returned to the chemical recovery cycle. The liquid fraction contains the main part of the potassium and chloride. One part of this liquid is discharged via the water treatment system and the remaining part is returned to the leaching tank, as illustrated in Figure 5. By adjusting the amount of recycled reject, the selectivity of the removal efficiency of Cl^- and K^+ and the recovery efficiency of Na_2SO_4 is controlled. Figure 7 shows a typical correlation between removal and recovery efficiency, based on units in operation. When the recycled fraction is decreased the removal efficiency of chlorides and potassium will increase. On the other hand the recovery efficiency of Na_2SO_4 will decrease. If instead the recovery of sodium and sulphate should be promoted the

amount of recycled liquid must be increased. This leads to a lower removal efficiency of chlorides and potassium since the bleed flow is decreased. This means that it is impossible to obtain maximum removal of chlorides and potassium at the same time as maximum recovery of Na_2SO_4.

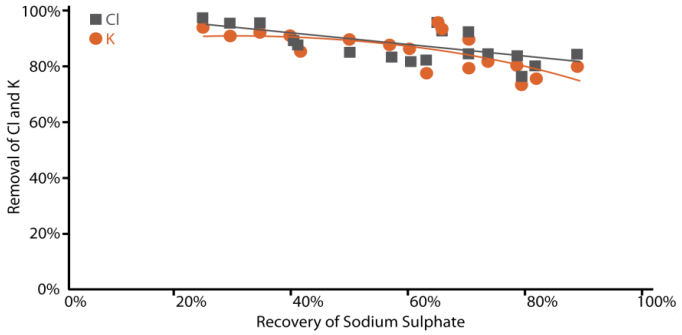

Figure 7. The removal efficiency of Cl^- and K^+ as a function of recovery efficiency of Na_2SO_4. The dots represent experimental data from different mills and the curves are regressions of the experimental data (15).

2.4 Solubility

A brief introduction to the thermodynamics of the dissolution of compounds is outlined in section 2.4.1 below. The solubilities of different compounds and mixtures common in the ESP ash are presented in 2.4.2. A limited number of studies have been done on concentrated inorganic salt mixtures common in forest industrial applications (17), for example mixtures containing ESP ash. The most interesting work performed by Goncalves, Jaretun, Linke and Teeple are presented in section 2.4.3.

2.4.1 Thermodynamics

The solubility of a compound in a solvent decides the number of compound molecules which can be dissolved to form a saturated solution. A sufficient amount of molecules must be dissolved to obtain equilibrium between the solvent and the undissolved solid. There are many different conditions which might affect the solubility of a compound in a pure solvent or solution, for example temperature, pH and composition. However, if one for example studies a two component system consisting of a partly soluble crystalline compound in water some important effects can be highlighted. When the equilibrium state for the two component system is obtained the dissolved compound molecules in the aqueous solution coexist with compound molecules bound to each other in solid phase (crystal). The concentration of dissolved molecules will then be unchanged with time. This means that the probability for a molecule to leave the solid state into solution must be the same as the probability to bind one dissolved molecule to the crystal. One important effect which contributes to the dissolution is the increased entropy when a molecule is mixed in the aqueous solution. However, this might be counterbalanced by the binding energy between molecules in the crystal. If the binding energy is large the probability for a molecule to leave the crystal is low resulting in low solubility. If the binding energy is low the probability for a molecule to obtain enough energy from the system to dissolve is much higher. If the temperature of the system is increased the available amount of energy increases which generally increase the compound solubility.

The balance between energy and entropy for the solvation process can be expressed by the difference in Gibbs free energy denoted ΔG between the aqueous phase and the crystal by expression:

$$\Delta G = G_{aq} - G_{Crystal} = \Delta H - T\Delta S \qquad (2.1)$$

where ΔH represents the enthalpy change and ΔS the entropy change for the solvation process at temperature T in degrees Kelvin. When equilibrium is obtained ΔG=0 and the net flow of molecules between the two different phases becomes zero. A closely related property to Gibbs energy is the chemical potential μ_i which

for a compound *i* in a multiple system of *j* components at constant pressure and temperature can be expressed as:

$$\mu_i = \left(\frac{\partial G}{\partial n_i}\right)_{P,T,j} \quad (2.2)$$

The chemical potential for a compound *i* can be related to a standard chemical potential μ_i° at a hypothetical standard state and the activity as:

$$\mu_i = \mu_i^\circ + RTlna_i \quad (2.3)$$

where R is the gas constant. The activity relates to the molar fraction as:

$$a_i = \gamma_i x_i \quad (2.4)$$

Here γ_i is the activity coefficient which contains the information about the deviation from an ideal dilute solution. When the concentration goes to zero the activity becomes equal to the molar ratio and the activity coefficient becomes equal to one.

When an uncharged hydrophobic compound is dissolved in water the aqueous solubility is low and can successfully be modelled by a simplified dissolution model based on an ideal dilute solution. It is assumed that a dissolved molecule is totally surrounded by water molecules and do not interact with other dissolved molecules. The molecular interactions within the crystal and the interactions between the solute and the water molecules are considered. For electrolyte systems the long range columbic forces between all charged ions must be considered already at very low concentration and will play a dominant role in the deviation from ideal solubility. Strong multiple electrolyte systems are common in pulp and paper industry. These systems become even more complex due to ion association, hydration, complex formation, and different precipitations taking place which must be taken into account (18) for proper predictions. It is also important to take the common ion effect in account. If a strong electrolyte is added to a solution with a weak electrolyte, where the strong and weak electrolytes have one ion in common, the solubility of the weak electrolyte is decreased as a result of the common ion effect (19). For example, when NaCl is present in aqueous solution, the solubility of Na_2SO_4 is decreased, since both salts consists of Na^+ (20). The short thermodynamic descriptions above must be adjusted for electrolyte systems due to the charge of dissociated ions etc. However this theory will not be further discussed in this thesis but good descriptions and summaries are found in literature (18).

2.4.2 Solubility in water

The solubilities of different salts normally present in precipitator ash dissolved in pure water are shown in Figure 8. As can be seen the solubilities for K_2SO_4 and KCl increase with temperature. The solubility of NaCl slightly increases with temperature (21). Na_2SO_4 and Na_2CO_3 solubilities increase rapidly between 0 – 40 °C but subsequently decreases between temperature of 40-100 °C. K_2CO_3 has a very high solubility between 50-60 wt% in water which might indicate that it is unlikely to precipitate even in mixtures. The solubility for the salts in pure water can be compared to the solubilities of the compounds in mixture discussed in section 2.4.3.

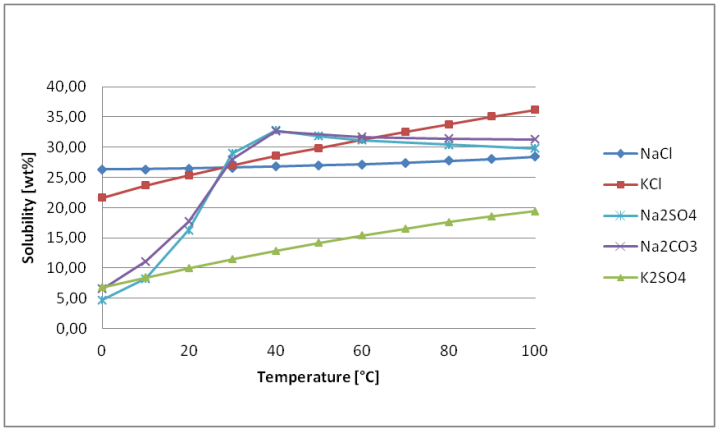

Figure 8. Solubilites of different anhydrous salts, common in the ESP ash, in pure water according to Perry, 1997 (21).

2.4.2.1 Solid phases

The desired composition of the ESP ash entering an ash leaching system is low content of potassium and carbonate and high content of Na_2SO_4 which leads to the formation of a recycled ash mainly composed of Na_2SO_4. This is not always the case since the ash composition might vary significantly between mills (11). When the potassium content increases, K_2SO_4 starts to precipitate which leads to formation of the double salts glaserite ($3K_2SO_4 \cdot Na_2SO_4$) (22). If the carbonate content increases, Na_2CO_3 will start to precipitate and form crystals together with Na_2SO_4, resulting in a double salt called burkeite ($2Na_2SO_4 \cdot Na_2CO_3$). Glaserite is formed when the potassium content of the slurry is high. K_2SO_4 precipitates together with Na_2SO_4 which leads to a lower removal efficiency of potassium and lower recovery efficiency of sodium. Figure 9 shows the transition between different solid phases depending on the potassium concentration and the molar ratio K/(K+Na) in the liquid phase.

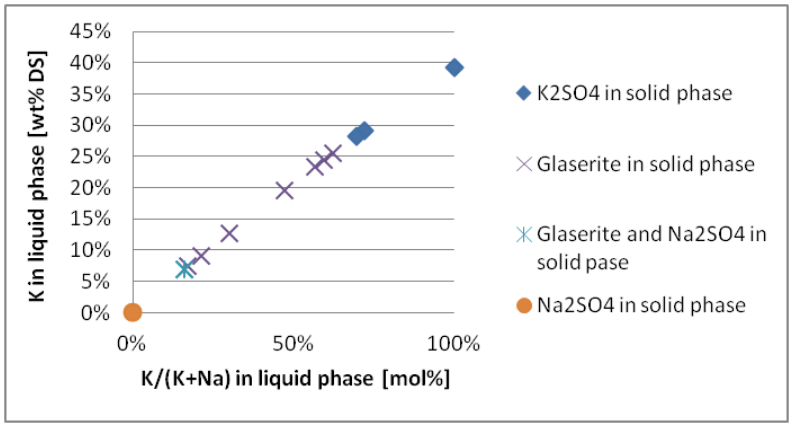

Figure 9. The transitions between different solid phases are shown in the figure, depending on the mass fraction of potassium, based on dry solids (DS), as a function of the molar ratio K/(K+Na) in the liquid phase (20). Data is taken for the system $Na_2SO_4 – K_2SO_4$ at 55 °C and are published in the work by Linke, 1958.

The potassium concentration in the liquid phase is usually quite low which means that Na_2SO_4 and sometimes glaserite are present in the solid phase. As shown in Figure 9 glaserite starts to precipitate at a concentration of 7 wt% potassium (based on dry solids in the liquid phase) in a mixed system of Na_2SO_4 and K_2SO_4 (20). The ash leaching process is usually operated with a potassium concentration between 0-12 wt% DS in the liquid phase. This means that either only Na_2SO_4 or glaserite and Na_2SO_4 probably should be present in the solid phase. By experience of the ash leaching plants the precipitation of potassium starts to become a problem when 11 wt%, based on dry solids (DS), potassium is present in the reject (15). The removal efficiency of potassium then decreases since it will precipitate as glaserite. Additional and more accurate data would be desirable to evaluate at what concentration glaserite starts to precipitate in the five component system Na^+- K^+- Cl^-- SO_4^{2-}- CO_3^{2-}. The precipitation of glaserite in the ash leaching process can be avoided by decreasing the recirculation and increasing the bleed until the concentration potassium is decreased in the system.

Burkeite results in two kinds of problems. It forms solid particles with a sticky character which increases the difficulties with dewatering the slurry suspension in the centrifuge. This leads to a lower removal efficiency of chloride and potassium since the recycled ash has a high liquid content. It will also affect the removal efficiency of sulphate, since burkeite will precipitate instead of the desired Na_2SO_4. From experience of units in operation the carbonate limit in the ESP ash is around 5 wt%. When the fraction is higher, burkeite starts to form and the result is a lower dry content in the recycled ash.

2.4.3 Solubility studies

In this section the most interesting studies published in literature are presented. It contains solubility experiments performed by Teeple, Jaretun and Goncalves. Data from the collocation with solubility experiments summarized by Linke is also presented.

2.4.3.1 Collocation of experimental data by Linke

The experimental data used in this project were gathered from the collocation of solubility experiments summarized by Linke year 1958 (20). All published results were experimentally determined and assembled for systems with no more than three components (20).

The most interesting systems for this thesis are Na_2SO_4 – NaCl, Na_2SO_4 - K_2SO_4 and Na_2SO_4 – Na_2CO_3, which have a major importance in the five component system Na^+- K^+- Cl^-- SO_4^{2-}- CO_3^{2-}. The systems Na_2SO_4- K_2SO_4 and Na_2SO_4 – Na_2CO_3 contribute to formation of glaserite respectively burkeite in the solid phase. As can be seen in Figure 10 and Figure 11, the solubility of different compounds change when other compounds are present in solution. In Figure 10 the difference in solubility of the mixture Na_2SO_4 - K_2SO_4 compared to the solubility of the pure compounds in water is shown. The solubility of K_2SO_4 is drastically decreased when Na_2SO_4 is added to the solution. Even for Na_2SO_4, the solubility is decreased in the mixture, but not as much as for K_2SO_4. This is due to the common ion effect and the fact that Na_2SO_4 is more soluble than K_2SO_4. A similar effect can be seen for the mixture of Na_2CO_3 and Na_2SO_4 where the solubility of Na_2CO_3 is drastically decreased compared to the solubility of the pure salt in water.

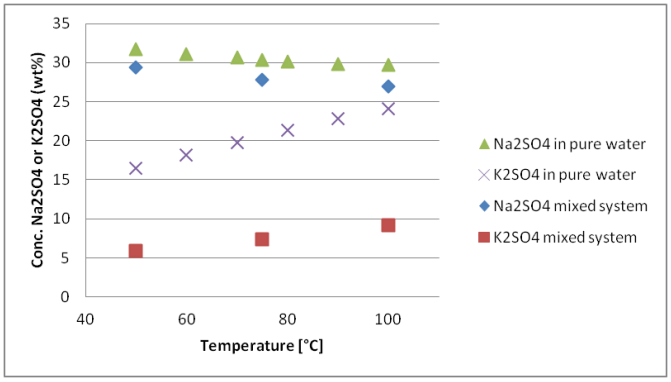

Figure 10. Solubilites of Na_2SO_4 and K_2SO_4 in the saturated system Na_2SO_4 - K_2SO_4 in water depending on temperature. The composition in the mixture is compared with the solubility of the pure compounds in water (20).

Figure 11 shows the solubilities of the saturated system NaCl - Na_2SO_4 which are compared to the solubility of the pure compounds in water. The solubility of both Na_2SO_4 and NaCl is decreased when mixed with each other. At a temperature of 90ºC NaCl precipitates at a concentration of 24,1 wt% and Na_2SO_4 at a concentration of 5,5 wt%. NaCl is more soluble than Na_2SO_4 and therefore the solubility of Na_2SO_4 decreases due to the common ion effect. The NaCl concentration in the reject in an ash leaching process is normally much lower than 24,1%, which means that the major part of the NaCl present will dissolve in solution.

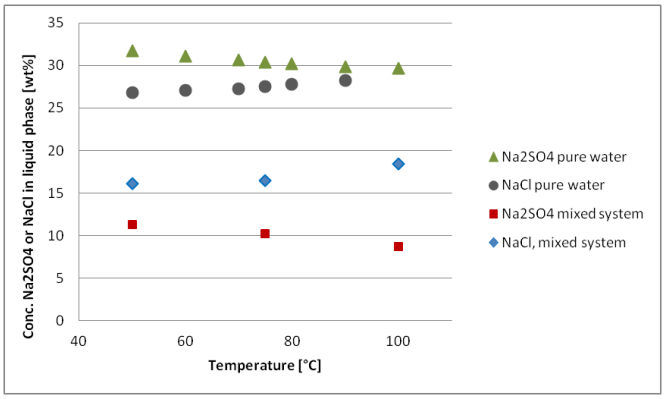

Figure 11. Solubilities for the system Na_2SO_4 – NaCl. The solution is saturated and in equilibrium with the solid phase consisting of Na_2SO_4 and NaCl. The solubilities for the pure compounds in water are shown for comparative purposes (20).

2.4.3.2 Experimental data produced by Teeple

When digging for gold in 1862, potash and borax where found in Searles Lake, a dry lake basin located in California. Later it was discovered that potash and borax were useful as detergents and for usage in cleaning products. In the early 1900's a separation plant was built in order to extract borax, potash, soda ash and Na_2SO_4. In 1929, John Teeple wrote a book about the salts of Searls Lake, with the objective to evaluate and improve the current plant. This was performed with experiments of the relative solubilities of the different salts and the influence of salts on the solubility of others. Some of his experiments include the same compounds as in precipitator ash, which makes his experiments interesting for this work (23).

Six interesting systems were investigated. One-five component and five four-component systems including NaCl, Na_2SO_4, Na_2CO_3, KCl, K_2SO_4 and K_2CO_3 are presented in Appendix B. All systems were dissolved in water and analysed at different temperatures. The five component systems were saturated with NaCl, which differ from the ESP ash in the sense that ESP ash is more likely to be saturated with Na_2SO_4 in solution. Since the operation temperature of the ash leaching process is around 80-90°C, the phase transitions at the higher temperatures is the most interesting. One of the most interesting systems is system V, containing Na_2SO_4, Na_2CO_3 and K_2SO_4 is presented in Figure 12. The solubilities of the three salts; Na_2SO_4, Na_2CO_3 and K_2SO_4 decrease in mixture compared to the solubilities of the pure compounds in water. The common ion effect makes burkeite and glaserite precipitate and the more soluble salt Na_2SO_4 dissolve in the solution. As can be seen the solubilities of Na_2SO_4 decreases and the solubility of Na_2CO_3 and K_2SO_4 increase within the temperature range of 50-75 °C. When comparing the composition K_2SO_4 in the system Na_2SO_4 - K_2SO_4 according to Linke to the system Na_2SO_4 - Na_2CO_3 - K_2SO_4 according to Teeple, shown in Figure 13, it can be seen that the data points conform relatively well. It can also be noticed that the linear trends in the mixtures is similar to the linear trend for K_2SO_4 in pure water, but with a shift in solubility of approximately 10 wt%, between the systems.

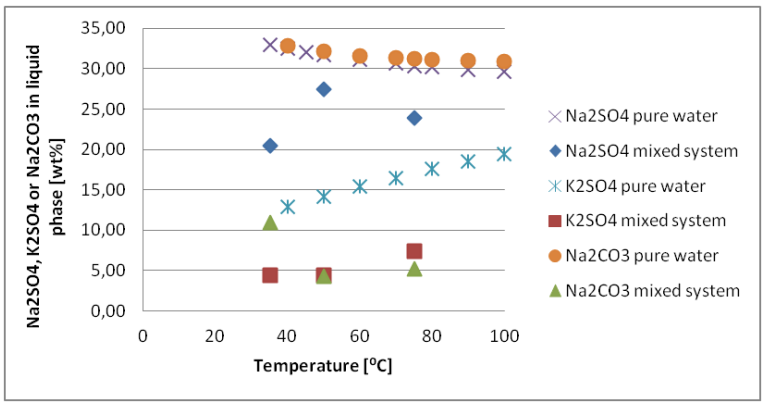

Figure 12. The solubility of individual salts (20, 21) and solubility of the mixture in the system Na_2SO_4 – Na_2CO_3 - K_2SO_4. The saturated solution is in equilibrium with the solid phase consisting of Na_2SO_4, glaserite and burkeite (23).

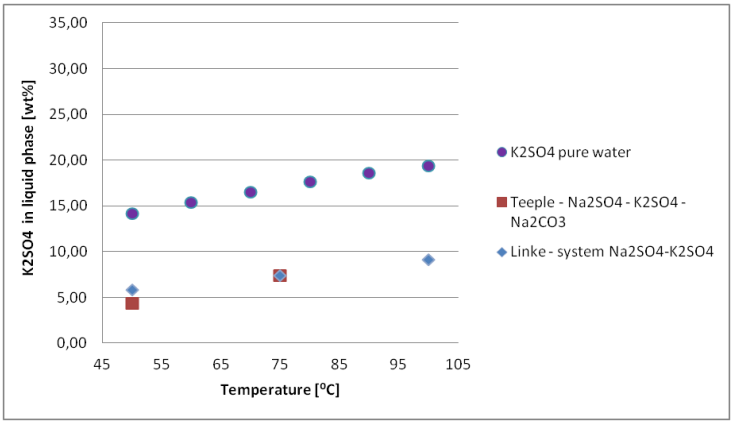

Figure 13. Solubility for K_2SO_4 in three different systems. The system of K_2SO_4 in pure water, the system Na_2SO_4-K_2SO_4 according to Linke (20) in equilibrium with the solid phase Na_2SO_4 and glaserite and the system Na_2SO_4 - Na_2CO_3-K_2SO_4 according to Teeple (23) in equilibrium with the solid phase Na_2SO_4, glaserite and burkeite.

2.4.3.3 Experimental data produced by Jaretun

The solubility of the five component system Na^+, K^+, SO_4^{2-}, Cl^- and CO_3^{2-} has been studied by Jaretun. One purpose of this study was to determine the solubility and removal efficiencies of chloride and potassium. Experiments using a synthetic precipitator ash were performed. The composition of the synthetic ash is shown in Table 2. This ash contains a very high amount of NaCl compared to a typical ESP ash shown in Table 1. The high concentration NaCl is chosen in order to determine the removal efficiency of chlorides at severe conditions (8).

Table 2. Synthetic ash composition in weight percentage.

Ash composition	*Percentage (wt%)*
Na_2SO_4	63
NaCl	29
Na_2CO_3	5
KCl	3

The setup of the experiment is shown in Figure 14. The temperature in the experiments has been varied between 55-75 °C. Results from the experiments are presented in Appendix B.

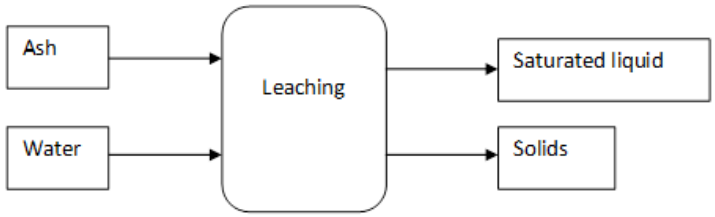

Figure 14. Schematic diagram showing the experimental setup used by Jaretun (8) and Goncalves (22).

The interesting results are that the temperature dependence for sodium and potassium seems to be negligible, as shown in Figure 15. But a slight temperature dependence can be seen for chloride and carbonate. The sulphate concentration decreases between 55 and 65 °C but at higher temperatures it seems to be independent of temperature. It is also noticed that the removal of chloride and potassium is high which gives a removal efficiency of 90-100%.

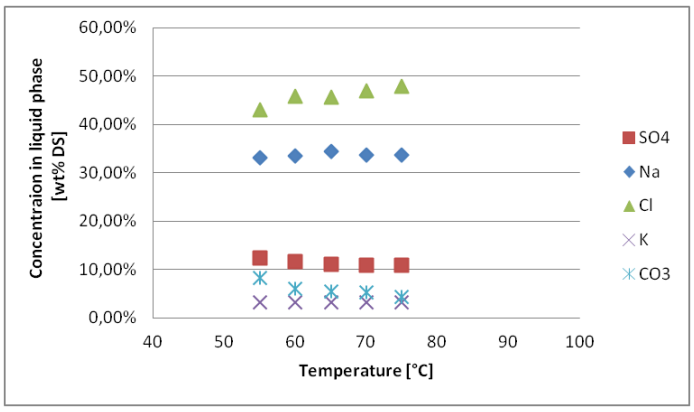

Figure 15. The composition of the synthetic precipitator ash in saturated solution analysed by Jaretun is shown in the figure. The ash content in the slurry are 1000 g ash /l water analysed in a temperature range of 55-75°C (8).

2.4.3.4 Experimental data produced by Goncalves

A laboratory study was performed by Goncalves in order to examine the main factors affecting the removal efficiency of chloride and potassium (22). The set up of the experiments was similar to the experiments performed by Jaretun, shown in Figure 14. Six different ash samples from four different mills, presented in Table 3 where investigated in the range of 60-100°C. This ash composition can be compared with the ash composition in Mill 1, Mill 2 and Mill 3 presented in Table 1. It can be noticed that the carbonate content is significantly higher in Mill 2 and Mill 3 than in the ash presented by Goncalves.

Table 3. Composition of different ESP ash samples used in solubility experiments performed by Goncalves.

Ash composition (wt%)	***Ash A***	***Ash B***	***Ash C***	***Ash D***	***Ash E***	***Ash F***
Na^+	29,30%	28,80%	31,50%	28,80%	27,80%	30,20%
K^+	5,60%	5,80%	5,20%	5,90%	6,70%	5,80%
Cl^-	6,60%	5,90%	5,40%	1,10%	3,40%	8,30%
CO_3^{2-}	1,20%	0,30%	12,40%	2,70%	0,10%	6,40%
SO_4^{2-}	56,90%	58,70%	45,50%	61,50%	61,50%	48,80%
Amount dissolved ash in liquid phase	30,07%	30,56%	29,87%	32,61%	32,80%	32,34%

The results showed that the removal efficiencies of chloride and potassium were directly proportional to the concentration of chloride and potassium in the slurry. No significant temperature effect was observed in the liquid composition of ash A as can be seen in Figure 16. The temperature dependence is slightly more linear than for Jaretun, but these experiments are performed at a higher temperature, which may affect the solubility.

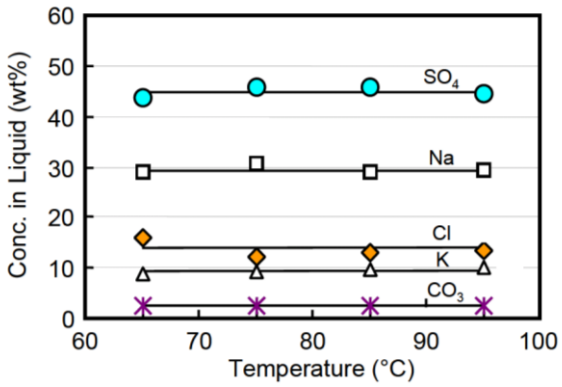

Figure 16. The temperature dependence of the composition in liquid phase (dry substance) of ash A, specified in Table 3, and an ash content of 800 g ash/l H_2O (22).

In Figure 17., the fraction of different ions is expressed as a function of the ratio ash to water in the slurry. As can be seen the sulphate concentration decreases as the chloride concentration, potassium and carbonate concentration increases. This means that higher ash content in the slurry increases the removal efficiency of sulphate, since less sulphate will dissolve. Therefore it is important to have a relatively high ratio ash to water in order to receive a high recovery efficiency of sulphate.

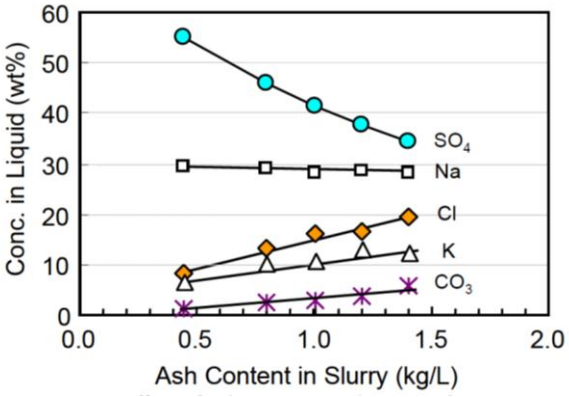

Figure 17. The liquid composition (dry substance) as a function of the ash to water ratio in the slurry of ash A at 85 °C (22).

2.5 Computational programs

This section gives a short description of the programs used during the thesis work. RBD is used for correction the experimental data in order to achieve electroneutrality and to predict the salt composition. The results predicted by Chemcad are used as a comparison with the developed models.

2.5.1 RBD

RBD (Recovery Boiler Design) is an in-house program developed by Metso Power, which is mainly used for the design of recovery boilers. It contains a data bank of literature data. These data can be used to calculate sticky temperature and composition of ashes containing sulphate, carbonate, chloride, potassium, sodium and sulfur. By specifying the amount of chloride, potassium and carbonate the fraction of sodium and sulphate can be calculated. The values are corrected in order to fulfill the criteria of electron neutrality. The composition of Na_2SO_4, Na_2CO_3, K_2SO_4, K_2CO_3, NaCl and KCl can then be predicted by the program.

2.5.2 Chemcad

Chemcad is a commercially available chemical process simulation software. It is mainly used to simulate chemical processes and can be used for both non electrolyte and electrolyte simulations. At Metso Power a standard module is used to predict the solubility of the different salt in the precipitator ash in water. The Pitzer electrolyte model is used to calculate the equilibrium of the salts in water. The model used assumes that only Na_2SO_4 is present in the solid phase, and that all other salts are completely dissolved. The calculation procedure starts by defining the ash composition (from RBD), water and ash flow. Then the amount recycled liquid and dry substance in recycled solids are specified. Finally the composition in slurry, reject and recycled ash is received.

3 Mass balances

The backbone of all of the models consists of mass balances describing the process and the individual components; leaching tank and centrifuge. Mass balances are based on the setup of the ash leaching process shown in Figure 18. Mass balances of the leaching tank are shown in equations 3.1 and 3.2. These balances are used to calculate the slurry flow and the flow of each component in the slurry. Similar balances for the centrifuge are shown in Appendix D, which gives the flow and composition of recycled ash.

$$\dot{m}_{slurry} = \dot{m}_{ash,in} + \dot{m}_{H_2O} + \dot{m}_{recirc.} \quad (3.1)$$

$$\dot{m}_{slurry} \cdot x_{i,slurry} = \dot{m}_{ash\ in} \cdot x_{i,ash\ in} + \dot{m}_{recirc.} \cdot x_{i,recirc.} \quad (3.2)$$

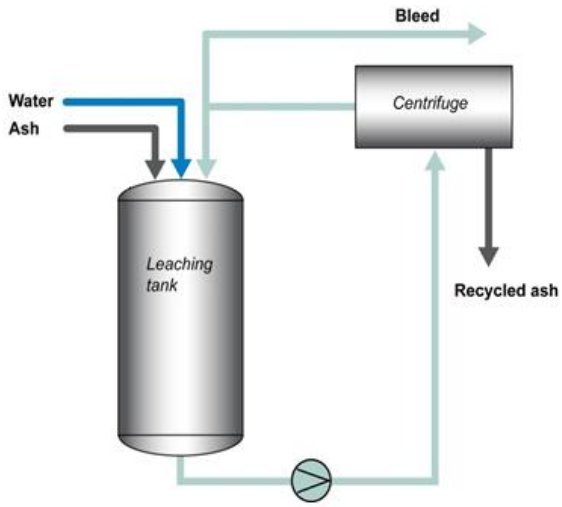

Figure 18. Schematic figure of the Metso AshLeach single stage system (15).

When the slurry is formed in the leaching tank, a fraction of the ash will dissolve in water and form a saturated solution. This means that the slurry consists of a saturated liquid phase which is in equilibrium with the solid phase, the suspended solids. The sum of suspended and dissolved solids equals the total amount of dry solids:

$$Total\ dry\ solids, DS = Dissolved\ solids, ds + Suspended\ solids, ss \quad (3.3)$$

The total amount of ESP ash dissolved in water is commonly considered to be 29 – 33 wt% in a saturated solution and depends among other factors on the ash composition. The amount of dissolved ash along with the solubility of different compounds is specified in each model. The main difference between the models is the prediction of the solubility of the compounds. The solubility is modeled using regression of experimental data. These relations will be discussed for each model in Chapter 4.

The amount ash dissolved depends on the total amount water in the leaching tank, as can be seen in Equation 3.4. The total amount water in the leaching tank includes the pure water flow and the water content in the recirculation flow.

$$\dot{m}_{dissolved\ ash} = \dot{m}_{H_2O} \frac{DS_{sat.sol.}}{1 - DS_{sat.sol.}} \quad (3.4)$$

$DS_{sat.sol.}$ is the dry solids content in a saturated solution, which by experience normally contains approximately 29-33% dry solids, as mentioned before.

This means that the amount water available decides how much ash that will dissolve. If the amount water is very high compared to the ash flow, it is possible to dissolve all ash present in the slurry. But since the aim is to remove chloride and potassium and recover sodium and sulphate, it is preferable to use a lower amount of water. This means that only a part of the ash will be dissolved whereas the rest will be present as suspended solids. The amount of suspended solids, ss, can be calculated by using the total content of dry solids, DS, in the slurry and the content dry solids in the saturated liquid phase:

$$ss = DS - (100 - DS)\left(\frac{DS_{sat.sol.}}{100 - DS_{sat.sol.}}\right) \quad (3.5)$$

The slurry is pumped to the centrifuge where the suspended solids are separated from the reject. For all models it is assumed that all suspended solids will be present in the recycled ash, which means that the separation in the centrifuge is total. The reject is consequently assumed to be a liquid without any suspended solids, as shown in Figure 6. In a plant with a centrifuge that is working properly it is a good assumption. Since it is difficult to separate all of the liquid from the solid phase in the centrifuge, the recycled ash will contain some liquid. As mentioned in section 2.3 the particle size and the mechanical work of the centrifuge, among other factors, affects the dryness of the recycled ash. The dryness of the ash is not investigated in this work and therefore the amount of suspended solids in the recycled ash must be specified in the models.

The Excel solver is used to solve the total mass balance, equation 3.6 and the mass balances for each compound, equation 3.7 over the process.

$$\dot{m}_{ash,in} + \dot{m}_{H_2O} - \dot{m}_{bleed} - \dot{m}_{rec.\ ash} = 0 \quad (3.6)$$

$$\dot{m}_{ash\ in} \cdot x_{i,ash\ in} - \dot{m}_{bleed} \cdot x_{i,bleed} - \dot{m}_{rec.\ ash} \cdot x_{i,rec.ash} = 0 \quad (3.7)$$

When the mass balances are solved the removal and recovery efficiencies can be calculated. The efficiencies are calculated as the ratio of the amount of a compound in the recycled ash divided by the amount of the compound in the incoming ash. Since the removal efficiency is mainly interesting for chlorides and potassium it is calculated by subtracting the recovery efficiency from the maximum efficiency, of 100%.

$$Cl^- \ removal = 1 - \frac{\dot{m}_{Cl,rec.ash}}{\dot{m}_{Cl,ash\ in}} \quad (3.8)$$

$$K^+ \ removal = 1 - \frac{\dot{m}_{K,rec.ash}}{\dot{m}_{K,ash\ in}} \quad (3.9)$$

$$Na^+ \ recovery = \frac{\dot{m}_{Na,rec.ash}}{\dot{m}_{Na,ash\ in}} \quad (3.10)$$

$$SO_4^{2+} \ recovery = \frac{\dot{m}_{SO_4,rec.ash}}{\dot{m}_{SO_4,ash\ in}} \quad (3.11)$$

$$CO_3^{2+} \ recovery = \frac{\dot{m}_{CO_3,rec.ash}}{\dot{m}_{CO_3,ash\ in}} \quad (3.12)$$

3.1 Comparison between predicted and experimental data

In order to compare the predicted results from the models with the experimental data, adaptations have been made. The calculation procedure is shown detail in Appendix D. These values have been calculated by using mass balances with the measured slurry flow and recirculation ratio together with the analysed dry solids content in slurry, reject and recycled solids. The recirculation ratio is defined as the ratio between the recycled reject divided by the total reject stream, shown in Appendix D. When using experimental data performed by Goncalves the provided ratio between ash and water in the slurry can be used in the model, since there is no recirculation back to the leaching tank. No assumptions need to be made which makes this comparison more robust.

A weakness with the accuracy and relevance of the experimental data from units in operation is the time for sampling. The ESP ash, slurry, reject and recycled ash samples are taken at the same time without respect to the residence time in the different units in the process. This error can be minimized by doing the leaching tests in a laboratory when the exact composition of ESP ash is known.

3.2 Evaluation of model assumptions

To evaluate if the assumptions used in the model are valid, a total mass balance of the process has been performed in order to calculate the composition in the liquid phase using experimental data. The water and ingoing ash flow are the same values used as input values in the model and the calculation procedure for these flows are shown in Appendix D. These balances gives also the flow of recycled ash. When using these flows together with the experimental data of ingoing and recycled ash composition the bleed composition can be calculated. This calculated composition in saturated solution will be referred to as calculated composition by mass balances. This balance has been chosen due to the fact that the experimental of ingoing ash and recycled ash probably are easier to analyse since the dry content is significantly higher than in the reject. The result is shown in Figure 19 and Figure 20. As can be seen in the figures there is a difference between the experimental and the calculated values by mass balances for all compounds in Mill 1, and mainly for chloride and carbonate in Mill 2. This implies that there are errors in the experimental data or that the assumptions are incorrect. Investigations about the assumption that no suspended solids are present in the reject needs to be evaluated. If suspended solids are carried over to the reject, the fractions of sodium and sulphate will increase whereas the fractions of chloride and potassium will decrease in the reject, which is the case in Mill 1. It would also be preferable to use additional and more accurate experimental data, since systematic errors might occur in the experimental work.

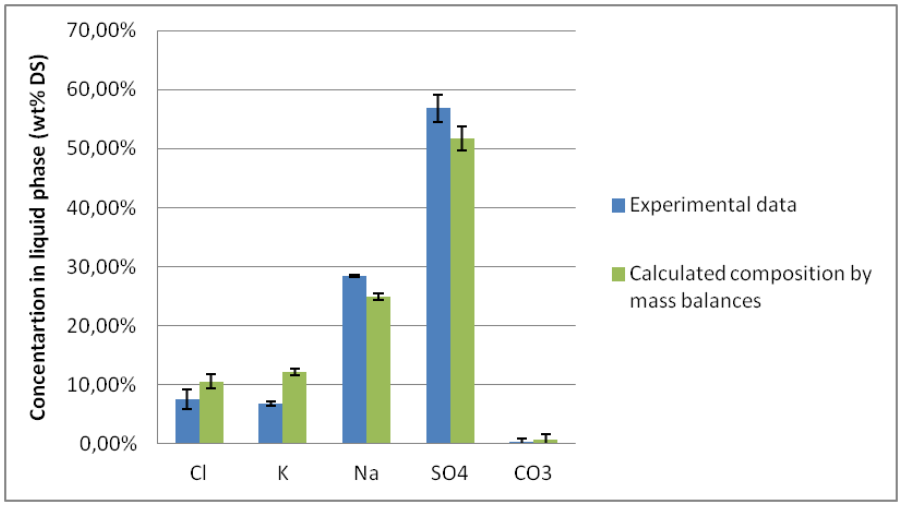

Figure 19. Comparison of reject composition when using experimental data and calculated composition by mass balances from Mill 1. The composition is in wt% dry solids in reject. Bars are average values and the error bars the standard deviation.

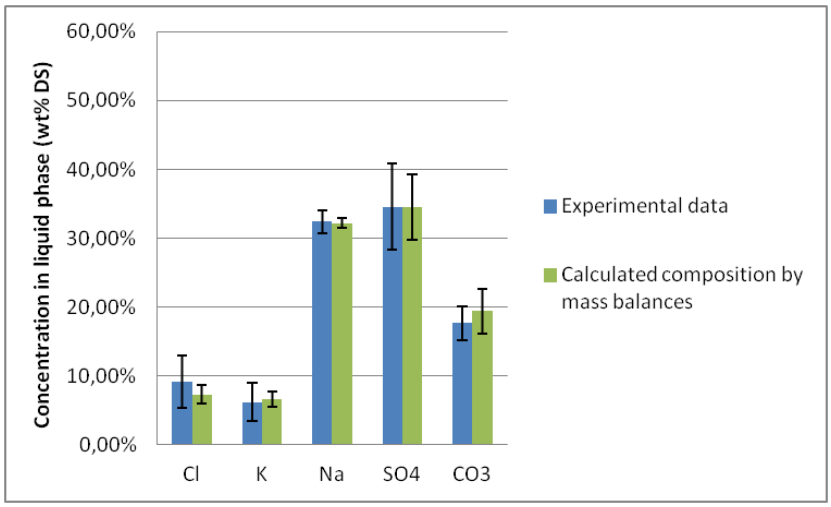

Figure 20. Comparison of reject composition when using experimental and calculated composition using mass balances in Mill 2. The composition is in wt% dry solids in reject. Bars are average values and the error bars are the standard deviation.

4 Models

The models have the same structure and are built mainly by mass balances presented in Chapter 3 and by regressions of experimental data from units in operation and literature data by Teeple, Jaretun and Goncalves. The main focus has been to find relationships of the solubility for the different compounds in ESP ash in saturated solution. NaCl is assumed to be completely dissolved in saturated solution in both models.

4.1 Model I

A first model was developed, in order to investigate if a simple model could give an estimation of the solubility and efficiencies for different components present in the ESP ash. This model is built by mass balances of the process which is presented in Chapter 3 and in Appendix D. To model the solubility of the components in the ESP ash two additional assumptions have been made. The first is that only Na_2SO_4 will be present in the solid phase. All other salts are assumed to be completely dissolved and are therefore present in the liquid phase. Since the operation temperature for the ash leaching system is 70-90 °C and the solubilities for example Na_2SO_4 and Na_2CO_3 changes drastically at temperatures below 40 °C, the model is only valid for temperatures above 60 °C. According to Goncalves the system is independent of temperature in the temperature interval of 70-90 °C.

The second assumption is that a fixed amount of ash will be dissolved in water. The dissolved amount ash in water is commonly considered to be between 29-33 wt% in a saturated solution for units in operation without the addition of sulphuric acid to the leaching tank, shown in Figure 21. For the mills that add acid, the solubility of the ash increases and is between 33-35 wt%.

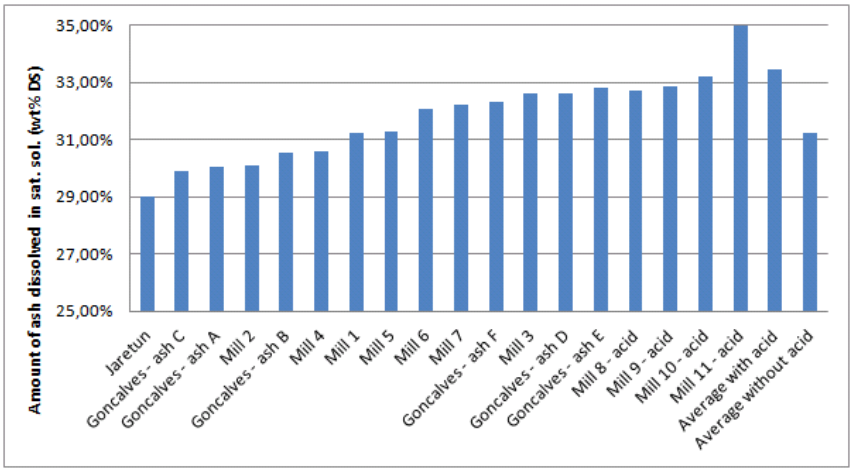

Figure 21. Amount of dissolved ash (wt%) in a saturated solution for ashes without and with addition of sulphuric acid, respectively. The experimental data is obtained from work performed by Goncalves and Jaretun and from different units in operation.

The average amount of dissolved ash without addition of sulphuric acid is 31,2 wt% and therefore the amount of dissolved ash in a saturated solution in the model will be fixed to 31 wt%. This means that the reject will consist of 31 wt% dry solids. As mentioned earlier, chlorides, potassium and carbonate are assumed to be completely dissolved. In order to add up to 31 wt% dissolved solids, sodium and sulphate are dissolved as well. The remaining Na_2SO_4 is present in the solid phase. The temperature dependence is not investigated. The Excel data sheet for calculations by Model I is shown in Appendix E

4.1.1 Input variables

The input variables used are ash and water flow, ash composition, recirculation ratio and amount of dry solids in centrifuge, all of which are presented in Table 4. Ash compositions and amounts of dry solids in the centrifuge are obtained from the experimental data and recirculation ratios from the process flows. In Model I the composition of ions are used as input variables and the Na_2SO_4 composition in the solid phase is calculated in the model by using molar weight for the different ions. Since only Na_2SO_4 is present in the solid phase, it is straight forward to calculate this composition and it is therefore possible to use single ions instead of salts as input values. Comparisons of experimental data from Goncalves, Mill 1, Mill 2 and Mill 3 are performed. The values of sodium and sulphate are corrected using the RBD software to achieve electroneutrality and a total amount of 100%, to make the experimental data possible to use in the model. When using the literature data obtained from Goncalves, only the solubilities of different compounds in saturated solution are predicted. According to the experimental setup, no liquid is recycled back to the leaching tank.

Table 4. Example of input data. The table shows one sample each from Mill 1 and Mill 2 and another sample performed by Goncalves. The experimental data is corrected in RBD in order to achieve electroneutrality. Additional data is presented in Appendix C.

	ESP ash composition from RBD		
Sample (wt% DS)	Mill 1 Ash sample 1	Mill 2 Ash sample 1	Goncalves Ash A
Cl^-	3,16%	4,24%	6,68%
K^+	4,30%	2,99%	4,92%
Na^+	29,63%	33,43%	29,32%
$SO4^{2-}$	62,90%	45,32%	57,86%
$CO3^{2-}$	0,01%	14,02%	1,22%
Suspended solids in centrifuge (wt%)	85,20%	56,52%	-
Recirculation ratio (%)	14,06%	27,32%	0%
Ash flow (kg/h)	5498	4808	800-1400
Water flow (kg/h)	4274	6438	1000

4.2 Model II

This model was developed in order to investigate if it is possible to use a system containing four components when describing the solubility of the ESP ash. The system Na_2SO_4 – Na_2CO_3 – K_2SO_4 is used. This system is chosen since the solubility of these salts is probably affected the most in the water and ash mixture. NaCl, KCl and K_2CO_3 have a high solubility and are probably completely dissolved, if the ash does not contain an abnormal content of these compounds. The assumption about the chlorides is made since the common ion effect drastically lowers the solubility of Na_2SO_4, Na_2CO_3 and K_2SO_4 in favour for dissolution of NaCl and KCl. The KCl concentration is usually quite low and will not exceed the limit when it starts to precipitate. The concentration of NaCl is higher, but still low enough for NaCl to stay in solution. The assumption is based on the system Na_2SO_4 – NaCl published by Linke. In this system, the solubility of NaCl is only slightly decreased while the solubility of Na_2SO_4 is drastically decreased in mixture compared to the solubility of the pure compounds in water. The same dependence is shown in the system containing KCl and K_2SO_4, where the solubility of K_2SO_4 is significantly decreased when KCl is present in the solution. The available data for K_2CO_3 is limited, but the salt has a very high solubility in water, between 50-60 wt% in a saturated solution. It is therefore assumed to be completely dissolved. Linear regressions of literature data published by Teeple in 1929 of the mixture Na_2SO_4 – Na_2CO_3 – K_2SO_4 in a saturated water solution are used. The regressions are functions of Na_2CO_3 and K_2SO_4, respectively, diluted in saturated solutions which are dependent on temperature. This means that fixed amounts of Na_2CO_3 and K_2SO_4 are dissolved in water at a specified temperature, and the remaining solids will be present in the solid phase.

The linear correlation used for K_2SO_4 is:

$$K_2SO_4\ (wt\%) = 0{,}0012T - 0{,}0154 \quad (4.1)$$

and for Na_2CO_3;

$$Na_2CO_3\ (wt\%) = 0{,}0003T + 0{,}0259 \quad (4.2)$$

Where T is the temperature in degrees centigrade. For example at 90 ºC the Na_2CO_3fraction in the liquid phase will be 5,3 wt% whereas the fraction K_2SO_4 will be 9,3 wt%.

NaCl, KCl and K_2CO_3 are assumed to be completely dissolved. The total amount dissolved ash are assumed to be 31 wt%. This means that Na_2SO_4 is dissolved until this value is reached. Data was unfortunately only available in the temperature range of 50-75 ºC, as shown in Appendix B. This regression is then extrapolated to 85 ºC when comparing the model with Goncalves and to 90ºC when comparing with Mill 1, Mill 2 and Mill 3. To investigate how the model affects the reject composition at different temperatures, predictions at 60, 70, 80 and 90ºC have been performed for Mill 1 and Mill 2.

4.2.1 Input variables

For Model II and for Chemcad, the salt composition and not only the composition of single ions are used as input values. Since more than one salt may be present in the solid phase it is important to know the amount of each salt present in the ingoing ash. This is due to the fact that the salt composition cannot be easy predicted in the model. As for Model I, ash and water flow, suspended solids in the centrifuge and recirculation ratio is used for Mill 1, Mill 2 and Mill 3. For Goncalves only the water flow together with ash flow and composition is specified in the models.

Table 5. Example of input variables. The table shows the ash compositions and process flows from literature data performed by Goncalves and experimental data from Mill 1 and Mill 2, where the experimental data is corrected in RBD in order to receive electroneutrality and to predict the composition of different salts in the ash. Additional data is presented in Appendix C.

	ESP ash composition from RBD		
	Mill 1 Ash sample 1	Mill 2 Ash sample 1	Goncalves Ash A
Na_2SO_4 (wt%)	85,69%	63,67%	76,14%
Na_2CO_3 (wt%)	0,02%	23,53%	1,91%
NaCl (wt%)	4,80%	6,64%	9,78%
K_2SO_4 (wt%)	8,97%	4,11%	10,49%
K_2CO_3 (wt%)	0,00%	1,61%	0,28%
KCl (wt%)	0,52%	0,45%	1,40%
Suspended solids in centrifuge (wt%)	85,20%	56,52%	-
Recirculation ratio (%)	14,06%	27,32%	0%
Ash flow (kg)	5498	4808	800-1400
Water flow (kg)	4274	6438	1000
Temperature (ºC)	60-90	60-90	85

4.2.2 Investigation of the amount ash dissolved with composition

The solubility of the ash changes with the ash composition among other factors. Therefore different amounts of ash dissolved in water have been used in Model II to predict the reject composition. This is done in order to investigate the dependence of the amount of dissolved ash in water on the composition in liquid phase. If the dissolved amount of ash in water is predicted to be too high, increased amount of Na_2SO_4 will dissolve which leads to a lower predicted removal efficiency of Na_2SO_4. Three different amounts of ash in water have been investigated: One regression is depending on the K/(K+Na) molar ratio in the slurry, shown in Figure 22, and two fixed amounts of ash at 31 wt% and 32 wt% dissolved solids in the liquid phase. The regression is based on literature data by Jaretun and Goncalves and it is a function of the amount of ash dissolved in water depending on the molar ratio K/(K+Na) in the slurry. The value of the correlation coefficient (R^2) is quite low and therefore a more accurate correlation would be desirable.

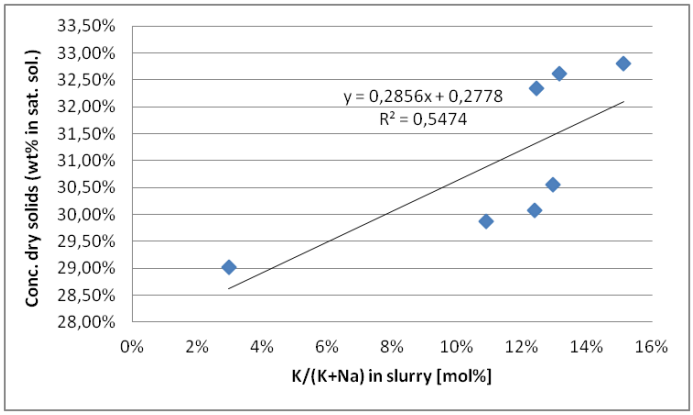

Figure 22. Amount of ash dissolved in water as a function of the molar ratio K/(K+Na) present in the slurry. Dots are experimental values according to Jaretun and Goncalves and the line is a linear regression of the experimental values.

The predicted results received by using the regression, 31 wt% or 32 wt% ash dissolved in saturated solution are compared to predicted values using the amount of dissolved ash specified in the experimental data. An example is shown below:

$$Difference_i = Model\ II\ (ash\ amount\ dissolved\ in\ liquid\ according\ to\ analysis)_i - Model\ II\ (31wt\%\ dry\ solids)_i \quad (4.3)$$

The difference between the predicted values for each compound i (Cl, Na, K, SO4 and CO3) is calculated for each mill.

5 Results and discussion

The outline of this chapter is first a comparison between the models without using recirculation. Thereafter the results when using recirculation are presented in section 5.2. In this section the temperature dependence by Model II is investigated. Finally, a comparison of predicted efficiencies by Chemcad and the different models are performed.

5.1 Predictions without recirculation

The ingoing ash composition together with the ratio ash to water in slurry according to Goncalves is used to predict the solubility in the liquid phase (without using recirculation and separation in the centrifuge). For both models an amount of dissolved ash in a saturated solution fixed to 31wt% has been used. As shown in Figure 23, both models predict a similar composition of Ash B (defined in Table 3) in the liquid phase. When comparing with the experimental data the chloride fractions are slightly larger and the potassium fractions are slightly smaller than in the experiments. This ESP ash contains a large fraction of sulphate and a minor fraction carbonate which makes it relatively straight forward to predict the composition in the liquid phase. Since there is no recycling of reject, all potassium salts in the slurry will probably dissolve. The larger fraction of potassium in the experiments compared to the predicted values is probably due to errors in the experiments, since the potassium is predicted to dissolve completely in the models.

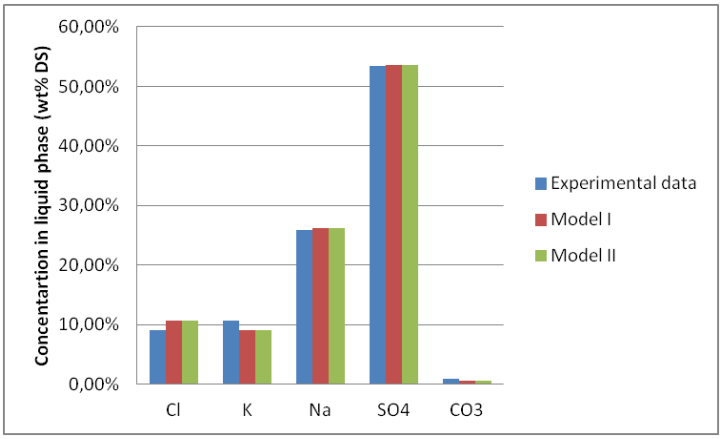

Figure 23.The composition in the liquid phase (wt% DS) for Ash B at 85ºC is shown for the experimental data and compared with the predicted values with the different models. The amount of ash in slurry is 800 g ash/l water. A fixed value of 31wt% dissolved solids is used for both models.

When using Ash C with an ash content in slurry of 500g ash/l water at a temperature of 85ºC to predict the composition in the liquid phase, the result looks a bit different. The potassium and chlorides should be completely dissolved according to the models in this case as well, but the experimental data shows a higher chloride and potassium value than the predicted values. This is probably due to experimental errors. Model II shows the best conformity with the experimental data for sodium, sulphate and carbonate, presented in Figure 24. Model I predicts larger fractions sodium and carbonate and smaller fraction sulphate when comparing with the experimental results. The poorer results for this ash compared to Ash B probably depends on the higher carbonate content present in the ESP ash which affects the composition in the solid phase and therefore also the composition in the liquid phase.

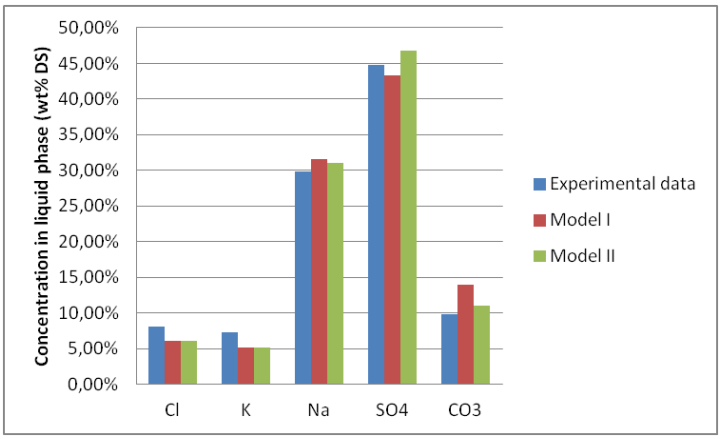

Figure 24. The composition in the liquid phase (wt% DS) for Ash C at 85ºC is shown for the experimental data and compared with the predicted values using three different models. The amount of ash in slurry is 800 g ash/l water. A fixed value of 31wt% dissolved solids is used for all models.

Experiments performed by Goncalves shows the variation in reject composition depending on the ratio of ash to water in the slurry. The models are used to predict the liquid composition at different ratios of ash to water in the slurry for Ash A. The predicted sodium and potassium fractions using Model I is shown in Figure 25. The predicted sodium concentration is generally lower than the experimental values and the predicted potassium concentration is generally higher than the experimental data. It can also be noticed that the experimental values of sodium level out as the ash content in the slurry increases. The predicted sodium and potassium concentration decreases respectively increases linearly and deviates more and more from the experimental data. This is because potassium is predicted to be completely dissolved in the Model I, which is not the case in reality. The fact that potassium is predicted to dissolve totally in the model leads to a lower predicted solubility of sodium. The composition predicted by Model II shows the same trend as Model I, which is shown in Appendix F. In Figure 26 the predicted concentration for different ratios of ash to water in slurry is shown. As can be seen the predicted values conform well to the experimental data in all points.

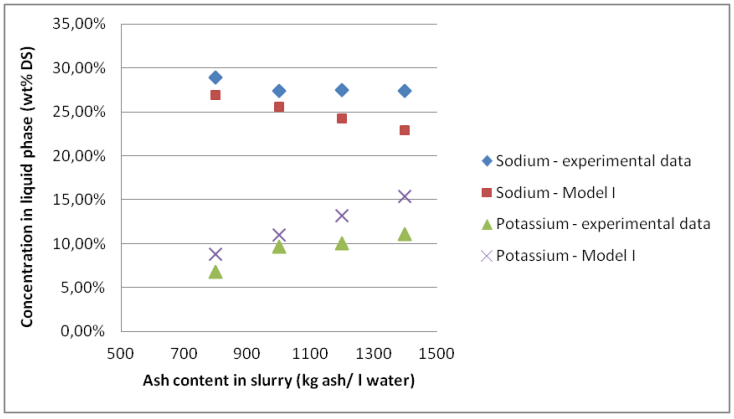

Figure 25. The composition in liquid phase (wt% DS) of Ash A depending on the ash content in slurry is shown in the figure. A comparison of the experimental data performed by Goncalves at 85ºC and the predicted values using Model I, with a dissolved ash amount of 31wt% in saturated solution is performed.

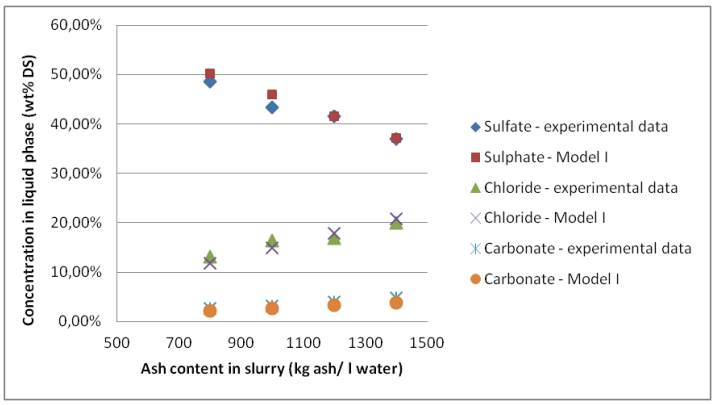

Figure 26. The composition in liquid phase (wt% DS) of Ash A depending on the ash content in slurry is shown in the figure. A comparison of the experimental data performed by Goncalves at 85ºC and the predicted values using Model I, with a dissolved ash amount of 31wt% in saturated solution is performed.

5.2 Predictions with recirculation

To evaluate how well the models predict the composition in the reject using recirculation and separation in a centrifuge, data from Mill 1 and Mill 2 have been utilised for predictions using Models I and II. As shown in Figure 27 the experimental data are not consistent with the predicted reject composition in Mill 1, but more consistent with the calculated composition using mass balances, defined in section 3.2 and Appendix D.

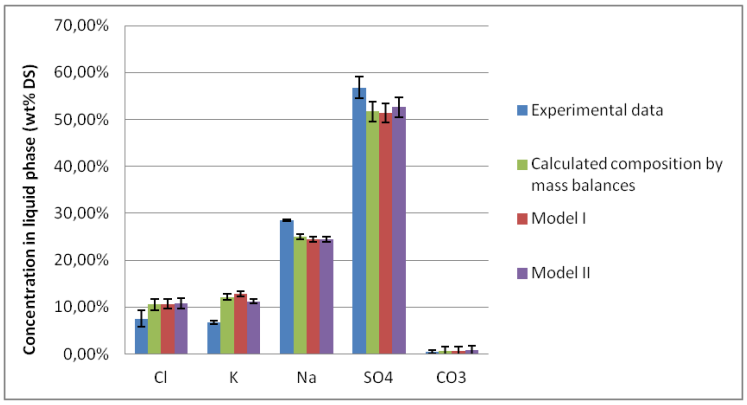

Figure 27. Reject composition in wt% dry substance of different ions present in the ash leaching process in Mill 1. The experimental data are obtained at 90ºC. A dissolved ash amount of 31 wt% ESP ash in saturated solution is used in the models. The bars show mean values of experimental data, calculated composition and predictions. The error bars shows the standard deviation of the mean values.

The chloride and potassium concentration in the reject is higher in Model I and II than in the reject analysis for Mill 1. But for both Models I and II the chloride fraction was consistent with the composition provided by the adjusted analysis. The opposite scenarios are shown for sodium and sulphate, with high values in the experimental data and lower values in the calculated reject data and predicted model results. The carbonate and chloride concentrations are low which means that they probably are completely dissolved, which is consistent with both models. In reality potassium may be present as glaserite which decreases the amount of potassium in the liquid phase, as predicted by Model II, where the potassium concentration is lower than that predicted by Model I. The fact that the composition of the reject obtained by the adjusted analysis is similar to that predicted in Mill 1 can probably be explained by the assumption that no suspended solids will be present in the reject. Suspended solids are carried over to the reject when the separation is performed in the centrifuge. This leads to a higher amount of Na_2SO_4 present in the reject, which means that the percental fractions of chloride and potassium will decrease in the reject.

The experimental data from Mill 2 shows that the amount of chloride is higher than the predicted values, shown in Figure 28. This should be impossible, since all chlorides are predicted to be completely dissolved in the model. This observation might therefore be due to uncertainties in the experimental data. However, when comparing the predicted values with the calculated values using mass balances data it gives a more consistent result.

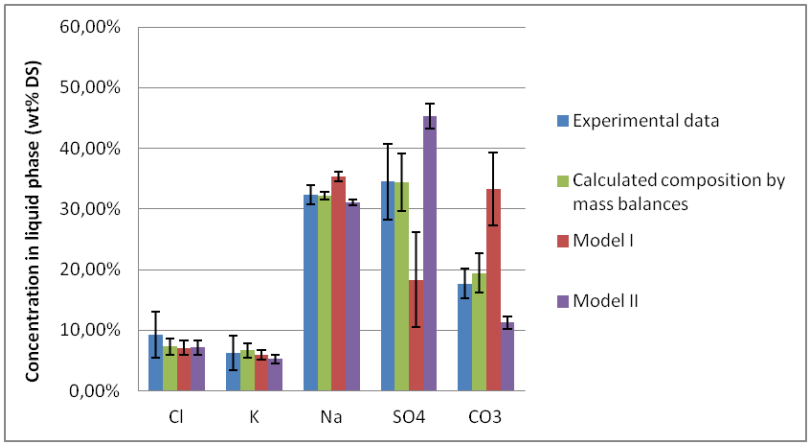

Figure 28. Composition in the reject, dry substance, of different ions present in the ash leaching process at Mill 2 at a temperature of 90ºC. The models assume that 31 wt% ash is dissolved in a saturated solution. Bars show mean values from experimental data and predicted values. The error bars show the standard deviation of the mean values.

The predicted and experimental data in the reject conform very well for potassium especially the values predicted by Model I with a small deviation for Model II. The big differences in sulphate and carbonate concentrations in the predicted values for Model I are due to the fact that only Na_2SO_4 is present as suspended solids in the model. For Model II the predicted values show the opposite result, where the sulphate concentration is very high in the reject compared to the experimental data and the carbonate concentration is lower than in the experimental data. In reality a significant amount of the double salt burkeite precipitates, but not as much as predicted by Model II. One of the ashes in Mill 2 had a carbonate concentration of 19,4 wt% DS. When carbonate content exceeds ~19 wt% DS in the slurry the predicted results by Model I becomes none physical due to limitations in the model as no carbonate will precipitate. The same result was predicted for Mill 3, where the carbonate concentration is even higher in the ash, 26,10 wt% DS. The result was a negative flow of sulphate in the liquid phase in Model I, as for Mill 2. If one wants to use this model further, the problem might be solved by letting Na_2CO_3 precipitate in order to add up for the Na_2SO_4 that could not precipitate.

When comparing the reject composition determined by experiments with the data predicted by the models the result conform very well for Mill 1, as can be seen in Figure 29. Since the incoming ash in Mill 1 mainly is composed of Na_2SO_4, it will also be the main component present in the recycled ash. The result was a bit different for Mill 2 compared to Mill 1, mainly due to the higher carbonate content in the ash. The results are presented in Figure 30. This figure shows that the sulphate content is higher for Model I and lower for Model II when compared to the experimental data. The opposite relation is shown for carbonate, where the predicted carbonate content in the recycled solids is low for Model I and high for Model II compared to the experimental data.

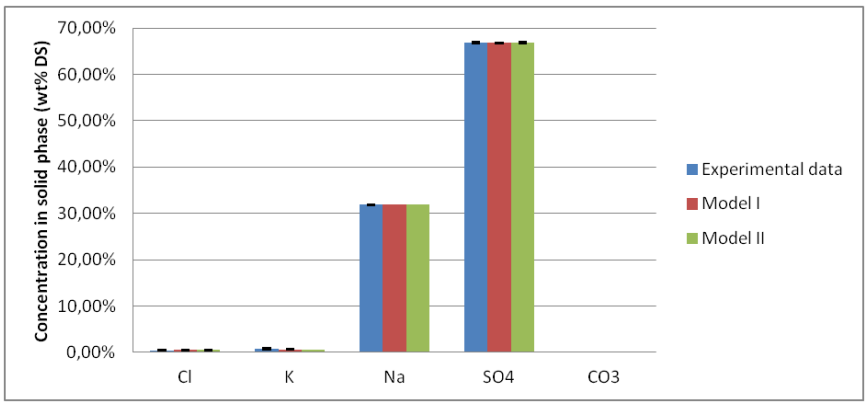

Figure 29. Comparison of experimental and predicted compositions of recycled ash in Mill 1. The composition is given as dry solids. The bars show the mean values and the error bars denote the standard deviations.

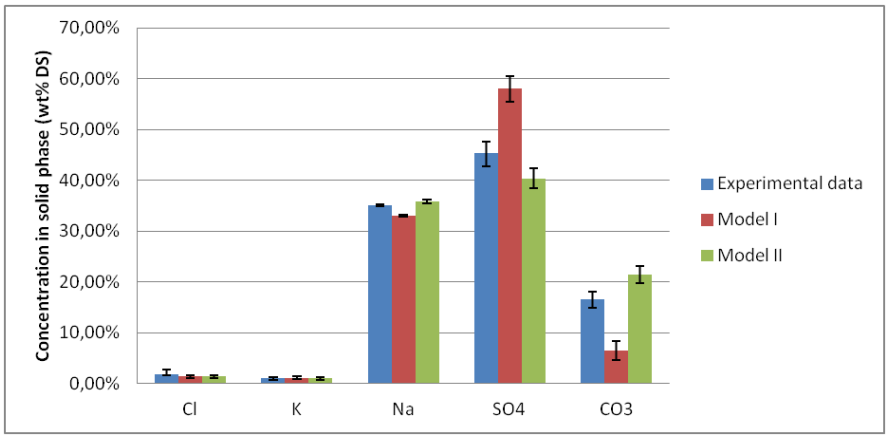

Figure 30. Composition in recycled ash presented as dry solids in Mill 2. Bars denote mean values whereas error bars denote the standard deviations.

5.2.1 Investigations of the ash amount dissolved

The regression determined by the experimental data performed by Jaretun and Goncalves, shown in Figure 22, is compared with experimental data in the reject from Mill 1, Mill 2 and Mill 2 (Figure 31). The data points are unevenly distributed and only one point coincide with the regression.

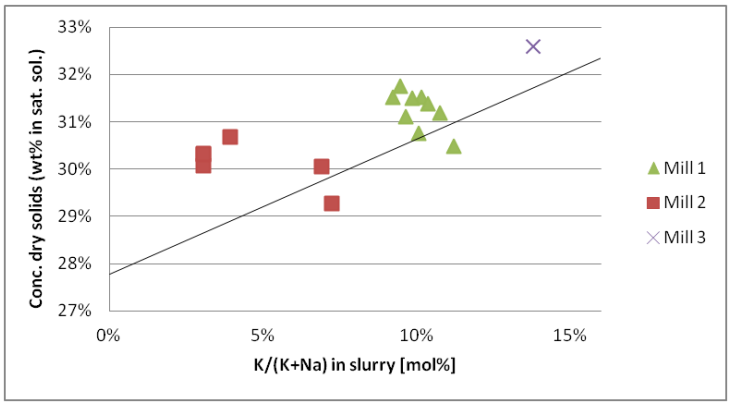

Figure 31. Experimental data of dry solids in liquid phase from Mill 1, Mill 2 and Mill 3. The straight line is a regression from literature data performed by Jaretun (8) and Goncalves (2, 22).

The deviations between the predicted values using dry solids according to reject analysis and the predicted compositions using 31 wt%, 32 wt% and the regression according to Jaretun and Goncalves is presented in Table 6. The maximum average deviations are shown for each mill. Mill 3 shows the largest deviation, which is because of the high dissolved ash amount in this mill, 32,6 wt% according to experimental data. The result is a deviation that varies between 0,2-2,3 wt%. The regression gives slightly better predictions, but there are still deviations. The same procedure has been performed for the efficiencies. It is consequently investigated how much the dissolved ash amount in the liquid phase influences the efficiencies. As presented in Table 7 the deviations between efficiencies vary from 0,5 to 9,2%. A deviation of 9,2 % shows that the solubility of the ash may give a significant error on the efficiency of the plant.

Table 6. The table shows the maximum deviation from the predicted composition in the reject by using Model II with a dissolved ash amount corresponding to the experimental data compared to predicted values using a dissolved ash content in a saturated solution of 31 wt%, 32 wt% or by the regression according to Jaretun and Goncalves.

	31 wt%	***32 wt%***	***Regression Jaretun & Goncalves***
Mill 1	± 0,2 %	± 0,5 %	± 0,6 %
Mill 3	± 2,3 %	± 0,8 %	± 1,6 %
Mill 2	± 0,8 %	± 1,7 %	± 0,5 %

Table 7. The table shows the maximum deviation from the predicted efficiencies by using Model II with a dissolved ash amount corresponding to the experimental data compared to predicted values using a dissolved ash content in saturated solution of 31 wt%, 32wt% or by the regression according to Jaretun and Goncalves.

	31 wt%	***32 wt%***	***Regression Jaretun & Goncalves***
Mill 1	± 0,5 %	± 1,2 %	± 1,3 %
Mill 3	± 5,3 %	± 2,0 %	± 3,9 %
Mill 2	± 5,5 %	± 9,2 %	± 1,0 %

Due to the deviations shown more effort should be put into finding a more accurate correlation of the amount of dry solids dissolved in water. This correlation is only dependent on the molar ratio of K/(K+Na) in the slurry which is an rough approximation. The synthetic ash used by Jaretun had low potassium content but high content of chloride. Such high amounts chloride probably affected the solubility and resulted in a dissolved ash amount of approximately 29 wt % in saturated solution, which might be lower than if lower amounts of chloride would have been present.

5.2.2 Temperature dependence of Model II

The effect of the temperature dependence in Model II was investigated by making predictions of the reject composition in Mill 1, Mill 2 and Mill 3 in a temperature range of 60-90ºC, using a fixed amount of 31 wt% ash dissolved in a saturated solution. The predicted result for Mill 3 is shown in Figure 32 and can be compared with the results published by Goncalves. According to Goncalves no temperature dependence can be seen when predicting the reject composition using ash A, which is shown in Figure 16. The predictions made by Model II diverge from the literature data presented by Goncalves since a slight temperature dependence on sulphate and carbonate concentrations occurs, which is shown in Figure 32. The ESP ash produced in Mill 3 contains high amounts of carbonate and therefore a temperature dependence of carbonate can be seen, since a fixed amount carbonate is dissolved at a given temperature. The carbonate content increases whereas the potassium content decreases with temperature. A similar dependence can be seen for Mill 2, which also has high contents carbonate in the ash. A dependence on potassium and sodium can be seen in the Mill 1 mill, shown in Appendix G. This depends on the higher amount of potassium present in the ESP ash in Mill 1. This divergence from the literature data according to Goncalves and Jaretun, means that it

might be difficult to model the five components system Na – K – Cl - CO_3 – SO_4 by merely using a four component system depending on temperature.

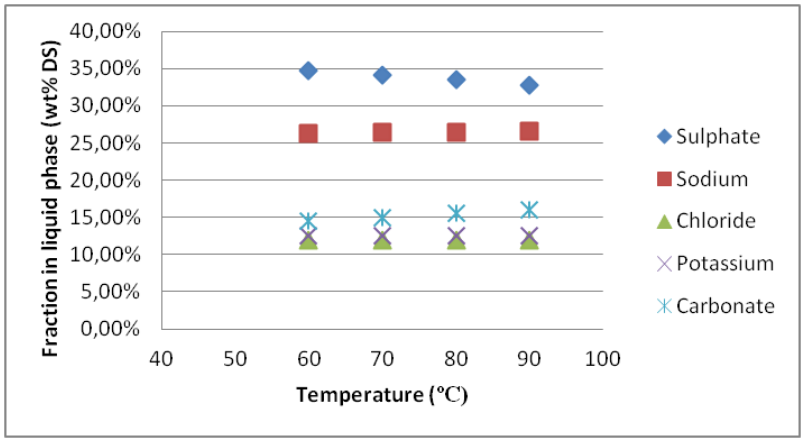

Figure 32. Temperature dependence predicted by Model II for Mill 3 in a temperature interval of 60-90°C. The model dissolves 31 wt% ash in a saturated solution.

5.3 Comparison with Chemcad

A comparison between Model I, Model II and Chemcad is performed. Simulations of the different ash compositions from Mill 1, Mill 2 and the ash composition of Ash E according to Goncalves have been performed in Chemcad and corrected by the Excel worksheet used by Metso Power. For the mills, the same ESP ash composition and flow, water flow, recirculation ratio and suspended solids in the centrifuge as in the models are used in the Chemcad module. Examples of input data for Mill 1 and Mill 2 are specified in Table 5. For ash E an amount of suspended solids of 26 wt% in the slurry and 80 wt% in recycled ash are specified. The recirculation ratio are specified to 30, 50 and 70%.

The efficiencies calculated using the predicted composition in the recycled ash by Models I and II are compared with the efficiencies calculated using the corrected Chemcad predictions. The calculated efficiencies for Mill 1 are quite consistent with experimental data for both models, as shown in Figure 33. The result from Chemcad shows a lower removal efficiency for potassium and higher recovery efficiency of sodium, as presented in Figure 33.

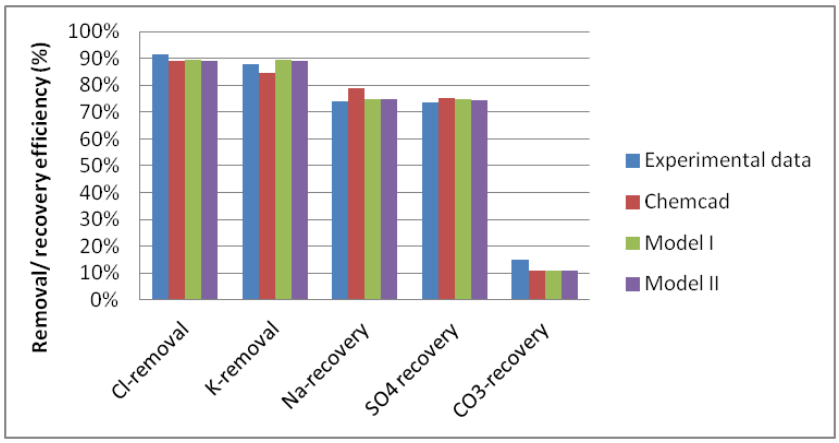

Figure 33. Comparison of the efficiencies based on experimental values and values predicted by Models I and II. The bars represent mean values from Mill 1. Chemcad simulations and predictions made using Model II are performed at 90°C.

For Mill 2 the efficiencies predicted by the models show a larger deviation from the efficiencies calculated by the experimental data compared to the case of Mill 1. This deviation is conducted with the deviation between the experimental data and predicted data of the recycled ash, since the compound flows in the ingoing ESP

ash together with the compound flows in the recycled ash gives the efficiency for each compound. The differences in recovery efficiencies of sulphate and carbonate (Figure 34) comes from the fact that only Na_2SO_4 is assumed to be present in the solid phase in Model I, as mentioned earlier. This makes the predicted carbonate content much lower whereas the sulphate content becomes higher in the recycled ash compared to the experimental data which is presented in Figure 34 for Mill 2. The opposite relation is shown for Model I.

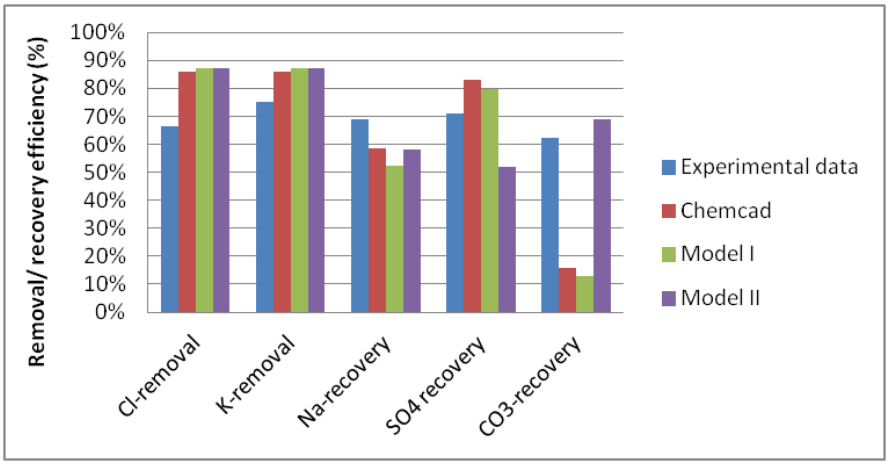

Figure 34. Comparison of the efficiencies based on experimental values and predicted values by Model I and II. The bars are average values from Mill 2. Chemcad simulations and predictions by Model II are performed at 90ºC.

To show the efficiencies for an ash consisting of a relatively high fraction potassium, Ash E according to Goncalves is used. Unfortunately no experimental data were available, but Model I and II have been compared to the corrected Chemcad data. In Figure 35 the efficiencies calculated by Model I, II and corrected Chemcad data are shown. It can be noticed that the recovery efficiency for potassium is low in the corrected Chemcad data and predicted data by Model II since these models take the precipitation of glaserite in account. This means that a increased amount of potassium will be present in the solid phase. In order to further investigate the accuracy of the glaserite precipitation, it is necessary to compare the results with experimental data.

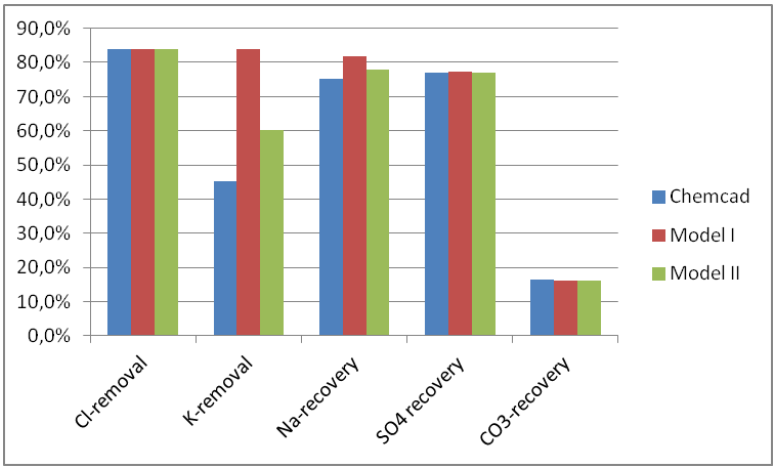

Figure 35. Comparison of the predicted efficiencies by Model I and II with corrected data by Chemcad of Ash E. A recirculation ratio of 50% and a suspended solids amount of 26 wt% in slurry have been used. The amount of suspended solids in the recycled ash are fixed to 80 wt% Chemcad simulations and predictions by Model II are performed at 90ºC.

5.3.1 Effect of recycling

When recirculation is used it affects the composition of the liquid phase and therefore also the composition of the solid phase. By comparing predictions by Model I, II and corrected data from Chemcad, the variations of potassium with recirculation ratio for Ash E can be seen in Figure 36. Three different recirculation ratios of 30, 50 and 70%, respectively, have been investigated. Ash E is as mentioned before an ash with relatively high content potassium and when the recirculation ratio is increased, the effect of the fraction potassium in the solid and liquid phase can be seen. For Model I, both the fraction potassium in liquid and solid phase increases, since potassium is predicted to be completely dissolved. For Model II and Chemcad the fractions of potassium in liquid phase are relatively constant whereas the fraction in solid phase increases. This is due to formation of glaserite in solid phase, which is included in these models. Unfortunately no experimental data was available for this ash.

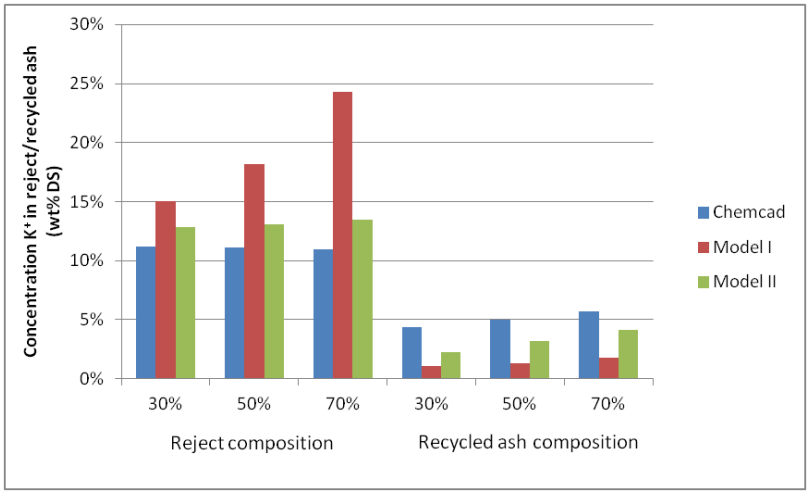

Figure 36. The potassium fraction in reject and recycled ash for Ash E according to Goncalves are predicted by Model I, II and corrected Chemcad predictions depending on the recirculation ratio. The recirculation ratio are fixed to 30, 50 and 70% at a temperature of 90ºC. The water flow is adjusted in order to achieve 26 wt% suspended solids in the slurry, which corresponds to ~50 wt% dry solids. The suspended solids in recycled ash are fixed to 80 wt%. In Model I and II the amount of dissolved solids was fixed to 31 wt%.

6 Conclusions

The assumption that all chlorides are dissolved in water is likely to be valid. Therefore the separation of chlorides are addicted to the dewatering of the recycled ash. More efforts are needed in order to determine the solubilities of Na_2SO_4, K_2SO_4 and Na_2CO_3 in mixture of ESP ash.

It is concluded that Model I predicts the composition for low carbonate and potassium ashes relatively well. But as the ash to water ratio or the carbonate content in slurry increase, the model deviates from the experimental data.

It will probably be difficult to predict the solubility of a precipitator ash only by using experimental data from the four component system $Na_2SO_4 – K_2SO_4 – Na_2CO_3$ dependent only on temperature, which is used in Model II. It would be preferable to expand the data range with experiments at higher temperatures, at least to 90ºC. A relatively accurate prediction of the reject composition can be made for an ash with low potassium and carbonate contents, but as these concentrations increase the results becomes more and more incorrect.

When using recirculation of reject back into the leaching tank, the predicted reject composition deviate from the experimental data. The deviation occurs for all compounds in Mill 1 and a significant deviation is shown for carbonate and sulphate content compared to experimental data obtained from Mill 2. When performing mass balances of the system in order to evaluate if the experimental data and assumptions are valid, it result in large deviations from the experimental data. These deviations likely depend on errors in the experimental data together with the assumption that no suspended solids are estimated to be present in the reject using the models. It is possible that carry over may occur in the centrifuge in reality, when the centrifuge does not work properly, which affects the performance of the ash leaching process.

When modelling different specified amounts of ash that are dissolved in a saturated solution, deviations occur when the results are compared with the predicted values using the specified amount of ash dissolved in the reject. The regression done using the experimental data according to Jaretun and Goncalves provides the most accurate results, but the results are not significantly better than in the case where the amount of dissolved ash is 31 wt% for the ashes investigated in this work. It is therefore important to find a more accurate correlation for the amount of dissolved ash in water.

It can also be concluded that the efficiencies predicted by Chemcad suffer from a quite similar deviation from those efficiencies based on the experimental data, just like the efficiencies calculated using the models. When studying the effect of recirculation ratio, both the corrected Chemcad data and predicted data by Model II shows an increasing amount of potassium in solid phase as the recirculation ratio increases. To further investigate the accuracy of these models, experimental data is needed for ashes containing a high content of potassium.

7 Future work

A larger quantity and more accurate data are needed to further evaluate the models. This data could also be used to evaluate the results predicted by Chemcad and when developing a thermodynamic model if this is desirable. Experiments with varied parameters like ash composition and ratio of ash to water in slurry are needed to further develop the models, in order to increase the accuracy. It may also be interesting to investigate the temperature dependence for an increased number of ashes in order to verify the results showing temperature independence according to Goncalves. Therefore it would be preferable to perform experiments in lab scale, maybe as a new Master's Thesis. Firstly, it should be advantageous to investigate the solubility of the ash according to the experimental setup used by Jaretun and Goncalves, as can be seen in Figure 14. Thereafter an ash leaching process in lab scale, consisting of a leaching tank and a centrifuge should preferably be performed. This setup provides data on how the recirculation of the reject will affect the composition in the recycled ash and reject. This setup may also provide an indication of which ash compositions that are likely to lead to carry over in the centrifuge, which results in suspended solids in the reject.

When using experimental data for calculations of process flows today, it is assumed that no suspended solids are present in the reject. To abandon this assumption it might be possible to use a statistical evaluation method such as the method of least squares predict the process flows. By using this kind of method it is also possible to evaluate the accuracy of the experimental data.

It should also be very interesting to investigate how different ash compositions affect the amount of dissolved ash and composition of different ions in a saturated solution. If more experimental data were available, the regression determined by data according to Goncalves and Jaretun could be evaluated further.

One way to further develop these models is to investigate if it is possible to use a model based on the molar ratio $CO_3/(CO_3+SO_4)$ or K/(K+Na) and the ratio ash to water in slurry to predict the composition of carbonate or potassium in the reject. The ratio K/(K+Na) is also important for the precipitation of glaserite, and need therefore to be investigated further.

The modelling of the dryness in the recycled ash coming from the centrifuge is not included in the developed models. This is an important parameter to take in account, since it will affect the efficiencies of the leaching process. Increased carbonate content results in formation of burkeite which decreases the particle size of the crystals, leading to a decreased ability to dewater the slurry. It might therefore be possible to use the dryness in the ash as a function of the carbonate content in the suspended solids to calculate the dryness in the centrifuge.

8 References

1. Knutsson M, Eriksson M, Sartório L. Experiences from first start-up of an ash leaching system. TAPPI Fall Conference & Trade Fair; San Diego, California, USA, 2002.

2. Saturnino D, Tran H. Prediction of the solubility of recovery boiler precipitator ash. TAPPI Journal. 2009.

3. Tran H, Earl P. Chloride and Potassium Removal Processes for Kraft Pulp Mills: A Technical Review. International Chemical Recovery Conference TAPPI/PAPTAC; June 7-10; Charleston, South Carolina, USA, 2004

4. Saturnino D, Cardoso M, Oliveira É. Dissolution of chloride and potassium salts during leaching of electrostatic precipitator ashes from kraft recover boilers. Appita Journal. 2009;62(1):52-9.

5. Saturnino D. The Solubility of Kraft Recovery Boiler Precipitator Ash. Toronto, Canada, : Graduate Departent of Chemical Engineering and Applied Chemistry, University of Toronto, 2006.

6. OLI, Systems, inc. OLI Electrolyte Simulation. www.olisystems.com.

7. Saturnino D. Personal Communication. 2012.

8. Jaretun A. Utstötning av klorid och kalium genom lakning av elektrostatfilteraska. Lund, 1998.

9. Tran H, Vakkilainnen E. The Kraft Chemical Recovery Process. Toronto, Cananda: 2008.

10. Johansson U. Different Methods for the Purge of Chlorides and Potassium from Electrostatic Precipitator Dust in the Kraft Mill. Stockholm, 2005.

11. Jordan J, Bryant P. Cluster Rule impact on recovery boiler operations : Chloride and potassium concentrations in the kraft liquor cycle. . TAPPI Journal. 1996;79(12):108-16.

12. Dahlbom J. Effekter av PFG vid indunstning och förbränning av bioslam i ett massabruks sodapanna. Stockhom.: Värmeforsk Service AB; 2003.

13. Minday M, Reid D, Burke M. An overview of various strategies for balancing saltcake, chloride and potassium level in an EFC kraft mill. TAPPI Minimum Effluent Symposium Oct. 23-24; San Fransisco, California, USA, 1997.

14. Ferreira L, Soares M, Egas A, Castro J. Selective removal of chloride and potassium in kraft pulp mills. TAPPI Journal. 2003;2(4):21-5.

15. Metso Power. Internal material. 2012.

16. Jaretun A, Aly G. Leaching of Chloride and Potassium from Electrostatic Precipitator Catch. International Chemical Recovery Conference, 1998.

17. Ahlroth M, Johansson U, Svedin K. Syntesrapport om kunskapsläget gällande löslighet och aktivitetsdata för högkoncentrerade saltlösningar i skogsindustriella tillämpningar. Stockholm, : 2007.

18. Jaretun A. Thermodynamic Modelling of Electrolyte Solutions with Application to the Pulp and Paper Industry. Alnarp: Förvaltningsavdelningens repro, SLU; 2000.

19. Mendham J, Denney RC, Barnes JD, Thomas MJK. Vogel's textbook of Quantitative Chemical Analysis 6th edition. Harlow, England: Pearson Education Limitied; 2000. 12-50 p.

20. Linke W. Solubilities, inorganic and metal organic compounds; a compilation of solubility data from the periodical literature. Fourth ed. Washington D.C., USA: American Chemical Society; 1958.

21. Perry H. Perry's Chemical Engineers' Handbook. Seventh ed: McGraw-Hill; 1997.

22. Goncalves C, Tran H, Shenassa R. Factors affecting chloride and potassium removal efficiency of a recovery boiler precipitator ash treament system. International Chemical Recovery Conference, PAPTAC & TAPPI; May 29 - June 1; Quebec, Canada, 2007.

23. Teeple J, E. The Industrial Developement of Searles Lake Brines. New York: The Chemical Catalogue Company; 1929.

Appendix A – Solubilities of anhydrous salts in water

Solubilities for single salts common in the ESP ash in pure water. Literature data according to Perry, 1997 and Linke, 1958.

Table 8. Solubility data for the system NaCl- H_2O at 0-100°C , Perry, 1997.

T (°C)	*g/100 g water*	*g/100 g saturated solution*	*Solid phase*
0	35,7	26,3	NaCl
10	35,8	26,4	NaCl
20	36,0	26,5	NaCl
30	36,3	26,6	NaCl
40	36,6	26,8	NaCl
50	37,0	27,0	NaCl
60	37,3	27,2	NaCl
70	37,8	27,4	NaCl
80	38,4	27,8	NaCl
90	39,0	28,1	NaCl
100	39,8	28,5	NaCl

Table 9. Solubility data for the system Na_2SO_4- H_2O at 35-100°C, Linke, 1958.

T (°C)	*g/100g water*	*g/100g satutated solution*	*Solid phase*
35	49,1	32,9	Na2SO4
40	48,1	32,5	Na2SO4
45	47,2	32,1	Na2SO4
50	46,4	31,7	Na2SO4
60	45,2	31,1	Na2SO4
70	44,2	30,7	Na2SO4
75	43,6	30,4	Na2SO4
80	43,2	30,2	Na2SO4
90	42,6	29,9	Na2SO4
100	42,2	29,7	Na2SO4

Table 10. Solubility data for the system Na_2CO_3 – H_2O at 40-100°C, Linke, 1958.

T (°C)	*g/100g water*	*g/100g satutated solution*	*Solid phase*
40	48,8	32,8	Na2CO3*H2O
50	47,5	32,2	Na2CO3*H2O
60	46,3	31,6	Na2CO3*H2O
70	45,6	31,3	Na2CO3*H2O
75	45,4	31,2	Na2CO3*H2O
80	45,2	31,1	Na2CO3*H2O
90	44,9	31,0	Na2CO3*H2O
100	44,7	30,9	Na2CO3*H2O

Table 11. Solubility data for the system KCl – H_2O at 0-100°C (21).

T (°C)	*g/100 g water*	*g/100 g saturated solution*	*Solid phase*
0	27,6	21,6	KCl
10	31,0	23,7	KCl
20	34,0	25,4	KCl
30	37,0	27,0	KCl
40	40,0	28,6	KCl
50	42,6	29,9	KCl
60	45,5	31,3	KCl
70	48,3	32,6	KCl
80	51,1	33,8	KCl
90	54,0	35,1	KCl
100	56,7	36,2	KCl

Table 12. Solubility data for the system K_2SO_4 – H_2O at 0-100°C, Perry, 1997.

T (°C)	*g/100 g water*	*g/100 g saturated solution*	*Solid phase*
0	7,4	6,9	K2SO4
10	9,2	8,4	K2SO4
20	11,1	10,0	K2SO4
30	13,0	11,5	K2SO4
40	14,8	12,9	K2SO4
50	16,5	14,2	K2SO4
60	18,2	15,4	K2SO4
70	19,8	16,5	K2SO4
80	21,4	17,6	K2SO4
90	22,8	18,6	K2SO4
100	24,1	19,4	K2SO4

Table 13. Solubility data for the system K_2CO_3 – H_2O at 0-100°C, Perry, 1997.

T (°C)	*g/100 g water*	*g/100 g saturated solution*	*Solid phase*
0	105,5	51,3	K2CO3*2H2O
10	108,0	51,9	K2CO3*2H2O
20	110,5	52,5	K2CO3*2H2O
30	113,7	53,2	K2CO3*2H2O
40	116,9	53,9	K2CO3*2H2O
50	121,2	54,8	K2CO3*2H2O
60	126,8	55,9	K2CO3*2H2O
70	133,1	57,1	K2CO3*2H2O
80	139,8	58,3	K2CO3*2H2O
90	147,5	59,6	K2CO3*2H2O
100	155,7	60,9	K2CO3*2H2O

Appendix B – Solubility for mixtures

Solubilities for mixtures published by Linke, Teeple, Goncalves and Jaretun.

Linke

Table 14. Solubility data for the system NaCl – Na_2SO_4 – H_2O at 50, 75 and 100°C, Linke, 1958.

	g/100 g saturated solution				
T (°C)	**NaCl**	**Na2SO4**	**Solid phase**	**Density (kg/m3)**	**Reference**
50	7,9	20,8	Na2SO4	1247	Chretien, 1926
	16,1	11,3	Na2SO4	1216	Chretien, 1926
	24,1	5,5	Na2SO4, NaCl	1223	Chretien, 1926
	25,4	2,6	NaCl	1203	Chretien, 1926
75	7,8	19,7	Na2SO4		Chretien, 1926
	16,5	10,2	Na2SO4		Chretien, 1926
	25,3	5,0	Na2SO4, NaCl	1207	Chretien, 1926
	26,4	2,1	NaCl	1189	Chretien, 1926
100	7,7	18,6	Na2SO4		Chretien, 1926
	18,4	8,8	Na2SO4		Chretien, 1926
	25,9	4,5	Na2SO4, NaCl	1194	Chretien, 1926
	27,2	1,8	NaCl	1777	Chretien, 1926

Table 15. Solubility data for the system Na_2CO_3 – Na_2SO_4 – H_2O at 50, 75 and 100°C, Linke, 1958. With solid phases C1=$Na_2CO3\cdot H_2O$, 1·2 = $Na_2CO_3\cdot 2Na_2SO_4$ (burkeite), SS = solid solution.

	g/100g saturated solution			
T (°C)	**Na2CO3**	**Na2SO4**	**Solid phase**	**Reference**
50	28,6	5,4		Dawkins, 1922
	28,5	5,9		Dawkins, 1922
	25,7	7,5		Dawkins, 1922
	19,4	12,9		Dawkins, 1922
	12,6	20,4		Dawkins, 1922
	10,5	22,5		Dawkins, 1922
	10,2	23,1		Dawkins, 1922
	5,1	27,3		Dawkins, 1922
	32,2	0,0	C1	Caspari, 1924
	29,7	5,5	C1, 1*2	Caspari, 1924
	11,4	22,2	1*2, Na2SO4	Caspari, 1924
	0,0	31,8		Caspari, 1924
75	31,5	0,0	C1	
	29,0	4,8	C1, 1*2	
	7,6	24,2	1*2, Na2SO4	
	0,0	30,4	Na2SO4	
100	30,8	0,0	C1	Green and Frattali, 1946
	29,6	2,1	C1	Green and Frattali, 1946
	28,8	3,4	C1, SS	Green and Frattali, 1946
	28,4	3,2	C1, SS	Green and Frattali, 1946
	28,6	3,4	C1, SS	Green and Frattali, 1946
	24,8	5,4	SS	Green and Frattali, 1946
	22,6	6,6	SS	Green and Frattali, 1946
	18,5	9,4	SS	Green and Frattali, 1946
	17,3	10,3	SS	Green and Frattali, 1946
	14,9	13,1	SS	Green and Frattali, 1946
	13,6	14,0	SS	Green and Frattali, 1946
	8,8	19,4	SS	Green and Frattali, 1946
	6,8	22,0	SS	Green and Frattali, 1946
	4,2	26,4	SS, Na_2SO_4	Green and Frattali, 1946
	2,9	28,0	Na_2SO_4	Green and Frattali, 1946
	1,5	28,3	Na_2SO_4	Green and Frattali, 1946
	0,0	30,0	Na_2SO_4	Green and Frattali, 1946

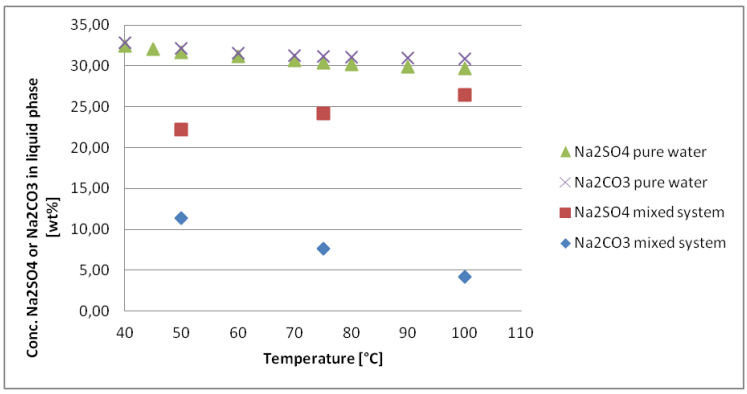

Figure 37. Solubilites of Na_2SO_4 and Na_2CO_3 in the saturated system Na_2SO_4 - Na_2CO_3 in water depending on temperature. The liquid phase is in equilibrium with a solid phase containing Na_2SO_4 and burkeite. The liquid composition of the mixture is compared with the solubility of the pure compounds in water, Linke, 1958.

Table 16. Solubility data for the system KCl – K_2SO_4 – H_2O at 50, 70, 75 and 100°C, Linke, 1958.

	g/100 g saturated solution				
T (°C)	**KCl**	**K2SO4**	**Density (kg/m^3)**	**Solid phase**	**Reference**
50	30,0	0,0	1198	KCl	Anosov and Byzova, 1947
	28,8	1,3	1204	KCl, K2SO4	Anosov and Byzova, 1947
	18,7	3,5	1143	K2SO4	Anosov and Byzova, 1947
	12,8	6,0	1123	K2SO4	Anosov and Byzova, 1947
	9,8	7,4	1120	K2SO4	Anosov and Byzova, 1947
	2,8	11,7	1115	K2SO4	Anosov and Byzova, 1947
	0,0	14,2	1112	K2SO4	Anosov and Byzova, 1947
70	32,6	0,0	1212	KCl	Anosov and Byzova, 1947
	31,3	1,4	1223	KCl, K2SO4	Anosov and Byzova, 1947
	30,0	1,8	1206	K2SO4	Anosov and Byzova, 1947
	22,2	4,1	1160	K2SO4	Anosov and Byzova, 1947
	13,4	7,8	1130	K2SO4	Anosov and Byzova, 1947
	8,9	10,1	1125	K2SO4	Anosov and Byzova, 1947
	3,8	13,7	1121	K2SO4	Anosov and Byzova, 1947
	0,0	16,6	1120	K2SO4	Anosov and Byzova, 1947
75	33,1	0,0	1203	KCl	Hering, 1926
	32,3	1,4	1211	KCl, K2SO4	Hering, 1926
	26,0	2,5	1171	K2SO4	Hering, 1926
	18,7	4,5	1135	K2SO4	Hering, 1926
	10,0	8,8	1110	K2SO4	Hering, 1926
	0,0	17,1	1116	K2SO4	Hering, 1926
100	36,1	0,0		KCl	Anosov and Byzova, 1947
	34,8	1,6		KCl, K2SO4	Anosov and Byzova, 1947
	34,4	1,8		K2SO4	Anosov and Byzova, 1947
	26,7	3,8		K2SO4	Anosov and Byzova, 1947
	22,1	5,3		K2SO4	Anosov and Byzova, 1947
	15,7	8,3		K2SO4	Anosov and Byzova, 1947
	9,5	12,4		K2SO4	Anosov and Byzova, 1947
	0,0	19,4		K2SO4	Anosov and Byzova, 1947

Table 17. Solubility data for the system Na_2SO_4 – K_2SO_4 – H_2O at 50, 70, 75 and 100°C, Linke, 1958. The formula of the solid phase glaserite is 3K2SO4·Na2SO4.

T (°C)	*g/100 g saturated solution*				
	Na2SO4	**K2SO4**	**Density (kg/m^3)**	**Solid phase**	**Reference**
55	0,0	15,0		K2SO4	Yanat'eva and Orlova, 1956
	5,1	14,5		K2SO4	Yanat'eva and Orlova, 1956
	5,6	14,3		K2SO4	Yanat'eva and Orlova, 1956
	5,6	14,3		K2SO4 "new" solid solution	Yanat'eva and Orlova, 1956
	6,0	14,1		"new" solid solution	Yanat'eva and Orlova, 1956
	6,7	14,1		"new" solid solution	Yanat'eva and Orlova, 1956
	7,4	13,6		Glaserite	Yanat'eva and Orlova, 1956
	8,1	13,1		Glaserite	Yanat'eva and Orlova, 1956
	8,8	12,8		Glaserite	Yanat'eva and Orlova, 1956
	11,6	11,6		Glaserite	Yanat'eva and Orlova, 1956
	19,0	9,1		Glaserite	Yanat'eva and Orlova, 1956
	24,9	7,5		Glaserite	Yanat'eva and Orlova, 1956
	28,0	6,5		Glaserite	Yanat'eva and Orlova, 1956
	29,0	6,2		Glaserite, Na2SO4	Yanat'eva and Orlova, 1956
	29,0	6,2		Glaserite, Na2SO4	Yanat'eva and Orlova, 1956
	31,6	0,0		Na2SO4	Yanat'eva and Orlova, 1956
50	29,4	5,9	1339	Glaserite, Na2SO4	Coenec and Krombach, 1928-1929
	5,68	13,8	1157	Glaserite, K2SO4	Coenec and Krombach, 1928-1929
75	27,8	7,4	1322	Glaserite, Na2SO4	Coenec and Krombach, 1928-1929
	5,6	16,4	1167	Glaserite, K2SO4	Coenec and Krombach, 1928-1929
100	27,0	9,2	1315	Glaserite, Na2SO4	Coenec and Krombach, 1928-1929
	5,5	18,8	1173	Glaserite, K2SO4	Coenec and Krombach, 1928-1929

Teeple

Table 18. Collocation of the systems investigated by Teeple, 1929.

System	*Salts*	*Temperature (°C)*
I	NaCl, Na_2SO_4, Na_2CO_3	20, 35, 50, 75, 100
II	KCl, K_2SO_4, K_2CO_3	35, 50, 75
III	NaCl, Na_2SO_4, KCl, K_2SO_4	20, 35, 50, 75, 100
IV	NaCl, Na_2CO_3, KCl, K_2CO_3	20, 35, 50, 75, 100
V	Na_2SO_4, Na_2CO_3, K_2SO_4, K_2CO_3	35, 50, 75
VI	NaCl (sat), Na_2SO_4, Na_2CO_3, KCl, K_2SO_4,K_2CO_3	20, 35, 50, 75, 100

Table 19. Solubility data for the system $Na_2CO_3 – K_2CO_3$ - Na_2SO_4 - $K_2SO_4 – H_2O$ at 35, 50 and 75°C, Teeple, 1929. The solid phase glaserite have the molecular formula $3K_2SO_4{\cdot}Na_2SO_4$ and burkeite $Na_2CO_3{\cdot}2\ Na_2SO_4$.

	g/100g H2O				*mole/1000 mole H2O*				
T (°C)	**Na2CO3**	**K2CO3**	**Na2SO4**	**K2SO4**	**Na2CO3**	**K2CO3**	**Na2SO4**	**K2SO4**	**Solid phase**
35	0,0	0,0	50,7	0,0	0,0	0,0	64,2	0,0	Na2SO4
	0,0	0,0	0,0	14,1	0,0	0,0	0,0	14,5	K2SO4
	48,8	0,0	0,0	0,0	82,9	0,0	0,0	0,0	Na2CO3*1H20
	0,0	115,1	0,0	0,0	0,0	150,0	0,0	0,0	K2CO3*3/2H2O
	0,0	0,0	48,8	7,9	0,0	0,0	61,8	8,2	Na2SO4, Glaserite
	0,0	0,0	7,2	15,0	0,0	0,0	9,2	15,5	K2SO4, Glaserite
	14,3	95,7	0,0	0,0	24,2	124,6	0,0	0,0	Na2CO3*1H20, Na2CO3*K2CO3
	9,3	108,8	0,0	0,0	15,8	141,7	0,0	0,0	K2CO3*3/2H2O, Na2CO3*K2CO3
	0,0	112,5	0,0	trace	0,0	146,5	0,0	trace	K2CO3*3/2H2O, K2SO4
	45,8	0,0	6,9	0,0	77,8	0,0	8,7	0,0	Na2CO3*1H20, Burkeite
	18,5	0,0	34,3	0,0	31,3	0,0	43,5	0,0	Na2SO4, Burkeite
	14,1	96,1	trace	0,0	24,0	125,2	trace	0,0	Na2CO3*1H20, Na2CO3*K2CO3, K2SO4
	9,1	108,9	trace	0,0	15,4	141,8	trace	0,0	K2CO3*3/2H2O, Na2CO3*K2CO3, K2SO4
	17,0	0,0	31,8	6,9	28,8	0,0	40,3	7,2	Na2SO4, Burkeite, Glaserite
	32,1	32,7	0,8	0,0	54,5	42,6	1,0	0,0	Na2CO3*1H20, K2SO4, Glaserite
	40,5	7,8	8,4	0,0	68,8	10,1	10,7	0,0	Na2CO3*1H20, Burkeite, Glaserite
50	0,0	0,0	46,6	0,0	0,0	0,0	59,1	0,0	Na2SO4
	0,0	0,0	0,0	17,1	0,0	0,0	0,0	17,6	K2SO4
	47,5	0,0	0,0	0,0	80,6	0,0	0,0	0,0	Na2CO3*1H20
	0,0	121,2	0,0	0,0	0,0	157,9	0,0	0,0	K2CO3*3/2H2O
	0,0	0,0	47,4	9,3	0,0	0,0	60,1	9,6	Na2SO4, Glaserite
	0,0	0,0	8,6	17,7	0,0	0,0	10,9	18,3	K2SO4, Glaserite
	15,8	95,2	0,0	0,0	26,8	124,0	0,0	0,0	Na2CO3*1H20, Na2CO3*K2CO3
	7,8	116,7	0,0	0,0	13,2	152,0	0,0	0,0	K2CO3*3/2H2O, Na2CO3*K2CO3
	0,0	121,2	0,0	trace	0,0	157,9	0,0	trace	K2CO3*3/2H2O, K2SO4
	44,4	0,0	6,3	0,0	75,4	0,0	8,0	0,0	Na2CO3*1H20, Burkeite
	12,6	0,0	36,7	0,0	21,4	0,0	46,5	0,0	Na2SO4, Burkeite
	15,2	95,2	trace	0,0	25,8	123,9	trace	0,0	Na2CO3*1H20, Na2CO3*K2C

									O3, K2SO4
	7,2	117,2	trace	0,0	12,3	152,6	trace	0,0	K2CO3*3/2H2O, Na2CO3*K2CO3, K2SO4
	6,8	6,9	43,1	0,0	11,6	9,0	54,6	0,0	Na2SO4, Burkeite, Glaserite
	29,9	38,1	1,1	0,0	50,8	49,6	1,5	0,0	Na2CO3*1H20, K2SO4, Glaserite
	38,0	10,3	8,7	0,0	64,6	13,4	11,1	0,0	Na2CO3*1H20, Burkeite, Glaserite
75	0,0	0,0	43,9	0,0	0,0	0,0	55,6	0,0	Na2SO4
	0,0	0,0	0,0	20,6	0,0	0,0	0,0	21,3	K2SO4
	45,3	0,0	0,0	0,0	77,0	0,0	0,0	0,0	Na2CO3*1H20
	0,0	136,4	0,0	0,0	0,0	177,7	0,0	0,0	K2CO3*3/2H2O
	0,0	0,0	44,4	11,7	0,0	0,0	56,3	12,0	Na2SO4, Glaserite
	0,0	0,0	8,1	21,8	0,0	0,0	10,3	22,6	K2SO4, Glaserite
	18,0	94,2	0,0	0,0	30,6	122,6	0,0	0,0	Na2CO3*1H20, Na2CO3*K2CO3
	5,1	133,5	0,0	0,0	8,6	173,9	0,0	0,0	K2CO3*3/2H2O, Na2CO3*K2CO3
	0,0	135,8	0,0	trace	0,0	176,9	0,0	trace	K2CO3*3/2H2O, K2SO4
	42,9	0,0	5,4	0,0	72,8	0,0	6,8	0,0	Na2CO3*1H20, Burkeite
	7,9	0,0	39,0	0,0	13,4	0,0	49,4	0,0	Na2SO4, Burkeite
	17,1	93,0	trace	0,0	29,0	121,2	trace	0,0	Na2CO3*1H20, Na2CO3*K2CO3, K2SO4
	4,8	133,5	trace	0,0	8,2	173,8	trace	0,0	K2CO3*3/2H2O, Na2CO3*K2CO3, K2SO4
	8,2	0,0	37,6	11,6	13,9	0,0	47,6	11,9	Na2SO4, Burkeite, Glaserite
	28,0	42,9	1,8	0,0	47,5	55,9	2,2	0,0	Na2CO3*1H20, K2SO4, Glaserite
	34,1	16,0	8,2	0,0	58,0	20,8	10,3	0,0	Na2CO3*1H20, Burkeite, Glaserite

Jaretun

Table 20. Original results from the leaching experiments according to Jaretun. The composition in liquid phase in a temperature interval between 55-75ºC, dependent on the ingoing ratio of ash to water are shown. Jaretun, 1998.

		Ingoing phase ratio (g/l)				
T (°C)	**Composition**	**600**	**800**	**1000**	**1200**	**1400**
55	K+ (M)	0,234	0,254	0,302	0,402	0,442
	Na+ (M)	5,550	5,464	5,732	5,680	5,620
	Cl- (M)	3,040	3,720	4,520	4,780	4,880
	CO32- (M)	0,352	0,434	0,494	0,540	0,482
	SO4 2- (M)	1,174	0,746	0,476	0,508	0,492
	Solution (g)	203,50	211,16	213,17	216,97	215,89
	Diluted solids (g)	62,02	64,14	69,17	72,02	73,77
60	K+ (M)	0,218	0,294	0,346	0,394	0,468
	Na+ (M)	5,298	5,716	6,046	5,660	5,520
	Cl- (M)	2,980	4,020	4,960	5,040	5,020
	CO32- (M)	0,372	0,496	0,510	0,392	0,378
	SO4 2- (M)	1,166	0,822	0,516	0,468	0,468
	Solution (g)	206,59	207,61	213,87	214,23	214,44
	Diluted solids (g)	60,89	63,88	68,43	70,49	71,16
65	K+ (M)	0,210	0,274	0,336	0,402	0,450
	Na+ (M)	4,916	5,298	5,568	5,706	5,480
	Cl- (M)	2,740	3,680	4,520	4,900	5,140
	CO32- (M)	0,316	0,408	0,410	0,348	0,316
	SO4 2- (M)	1,034	0,730	0,508	0,438	0,492
	Solution (g)	206,64	206,30	211,74	214,80	213,20
	Diluted solids (g)	60,96	62,90	67,32	72,20	70,37
70	K+ (M)	0,210	0,278	0,336	0,390	0,482
	Na+ (M)	4,984	5,402	5,532	5,638	5,360
	Cl- (M)	2,900	3,840	4,640	5,100	5,160
	CO32- (M)	0,342	0,442	0,434	0,344	0,252
	SO4 2- (M)	1,104	0,760	0,516	0,438	0,484
	Solution (g)	206,85	209,03	211,71	213,39	212,92
	Diluted solids (g)	60,56	63,75	67,16	69,72	69,49
75	K+ (M)	0,218	0,276	0,332	0,400	0,488
	Na+ (M)	5,064	5,290	5,716	5,680	5,560
	Cl- (M)	2,900	3,820	4,740	5,260	5,220
	CO32- (M)	0,350	0,422	0,374	0,286	0,246
	SO4 2- (M)	1,020	0,738	0,508	0,438	0,436
	Solution (g)	202,45	206,27	210,20	211,79	211,35
	Diluted solids (g)	58,62	62,40	65,92	69,98	70,59

The assumptions that were made to make it possible to calculate the composition in g/l H_2O was:

- That the water is taken at 25°C, with a density of 1000 kg/m^3.
- The dissolved material is calculated as weight of solution – 150 g water.
- The volume of solution can be calculated as;

$$V_{tot} = \frac{m_{tot}}{C_{Na} \cdot M_{Na} + C_K \cdot M_K + C_{SO4} \cdot M_{SO4} + C_{CO3} \cdot M_{CO3} + C_{Cl} \cdot M_{Cl}}$$

Goncalves

Table 21. Composition of different ash samples, calculated in RBD in order to receive electroneutrality and to calculate the composition of salts, Goncalves, 2007.

Ash composition (wt%)	***Ash A***	***Ash B***	***Ash C***	***Ash D***	***Ash E***	***Ash F***
Cl	6,68%	5,97%	5,46%	1,12%	3,45%	8,40%
K	4,92%	5,09%	4,60%	5,18%	5,87%	5,11%
Na	29,32%	28,92%	31,65%	28,77%	27,95%	30,39%
SO4	57,86%	59,70%	45,76%	62,20%	62,62%	49,62%
CO3	1,22%	0,30%	12,54%	2,74%	0,10%	6,48%
Na2SO4	76,14%	78,14%	61,15%	81,20%	80,16%	65,30%
Na2CO3	1,91%	0,47%	19,97%	4,26%	0,15%	10,16%
NaCl	9,78%	8,70%	8,12%	1,62%	4,91%	12,30%
K2SO4	10,49%	11,30%	7,25%	12,01%	13,86%	8,99%
K2CO3	0,28%	0,07%	2,52%	0,67%	0,03%	1,49%
KCl	1,40%	1,31%	1,00%	0,25%	0,88%	1,76%

Table 22. Reject composition for experiments performed by Goncalves at 85ºC.

Ash composition (wt% DS)	***Ash A***				***Ash B***	***Ash C***
	800g/l	**1000 g/l**	**1200 g/l**	**1400 g/l**	**800g/l**	**500g/l**
Cl	11,35%	16,40%	16,90%	20,00%	9,00%	8,10%
K	7,70%	9,70%	10,00%	11,10%	10,70%	7,30%
Na	28,65%	27,90%	27,90%	27,60%	25,90%	29,90%
SO4	49,40%	42,90%	41,30%	36,50%	53,50%	44,80%
CO3	2,85%	3,10%	3,90%	4,80%	0,90%	9,80%

Appendix C – Experimental data from units in operation

Mill 1

In this section the experimental data and corrected data by RBD for Mill 1 are presented. All samples are taken at a temperature of 90ºC.

Table 23. Experimental data of ash composition at Mill 1.

Experimental data	***Ash composition (wt%)***								
Sample	1	2	3	4	5	6	7	8	9
Cl	3,16%	2,95%	3,30%	3,70%	4,00%	4,10%	3,81%	3,85%	3,88%
K	4,30%	4,50%	4,40%	4,30%	4,20%	4,60%	4,40%	4,40%	4,20%
Na	29,30%	31,20%	30,57%	29,78%	30,59%	30,80%	30,73%	30,80%	30,74%
SO4	62,97%	64,19%	63,91%	62,49%	61,38%	61,32%	60,09%	62,54%	62,22%
CO3	0,01%	0,01%	0,05%	0,12%	0,84%	0,67%	0,18%	0,05%	0,17%
Dry solids	99,97%	99,96%	99,97%	99,92%	99,89%	99,95%	99,94%	99,97%	99,96%

Table 24. Ash composition calculated by the Recovery Boiler Design program developed by Metso Power. The experimental data of Cl, K and CO_3 are used, and the composition of Na and SO_4 are predicted by the program. Thereafter the program predicts the composition of different salts.

Calculated from RBD	***Ash composition (wt%)***								
Sample	1	2	3	4	5	6	7	8	9
Cl	3,16%	2,95%	3,30%	3,70%	4,00%	4,10%	3,81%	3,85%	3,88%
K	4,30%	4,50%	4,40%	4,30%	4,20%	4,60%	4,40%	4,40%	4,20%
Na	29,63%	29,47%	29,59%	29,72%	29,96%	29,65%	29,67%	29,65%	29,82%
SO4	62,90%	63,07%	62,66%	62,16%	61,00%	60,98%	61,94%	62,05%	61,93%
CO3	0,01%	0,01%	0,05%	0,12%	0,84%	0,67%	0,18%	0,05%	0,17%
Na2SO4	85,69%	85,58%	85,21%	84,71%	83,33%	82,63%	84,24%	84,39%	84,57%
Na2CO3	0,02%	0,02%	0,08%	0,20%	1,37%	1,08%	0,29%	0,08%	0,28%
NaCl	4,80%	4,46%	5,00%	5,62%	6,09%	6,19%	5,78%	5,84%	5,91%
K2SO4	8,97%	9,43%	9,14%	8,84%	8,42%	9,25%	9,01%	9,03%	8,59%
K2CO3	0,00%	0,00%	0,01%	0,02%	0,15%	0,13%	0,03%	0,01%	0,03%
KCl	0,52%	0,51%	0,56%	0,61%	0,64%	0,72%	0,64%	0,65%	0,62%

Table 25. Experimental data of slurry composition. Dry solids is the amount of diluted and suspended solids in the solution.

Experimental data	***Slurry composition (wt%)***								
Sample	1	2	3	4	5	6	7	8	9
Cl, %	3,06%	2,44%	3,01%	3,08%	4,01%	3,84%	4,06%	4,02%	3,74%
K, %	4,20%	4,50%	4,10%	4,60%	4,40%	4,80%	4,50%	5,00%	4,30%
Na, %	29,50%	29,40%	29,70%	29,80%	29,70%	29,50%	29,70%	29,40%	28,80%
SO4, %	63,74%	65,78%	64,03%	64,35%	63,28%	63,33%	62,72%	62,85%	64,22%
CO3, %	0,04%	0,02%	0,02%	0,03%	0,21%	0,43%	0,43%	0,33%	0,26%
Dry solids %	53,97%	54,93%	56,39%	54,62%	54,99%	53,53%	54,71%	54,92%	54,40%

Table 26. Slurry composition calculated by the Recovery Boiler Design program developed by Metso Power. The experimental data of Cl, K and CO_3 are used, and the composition of Na and SO_4 are predicted by the program. Thereafter the program predicts the composition of different salts.

Calculated from RBD	***Slurry composition (wt%)***								
Sample	1	2	3	4	5	6	7	8	9
Cl	3,06%	2,44%	3,01%	3,08%	4,01%	3,84%	4,06%	4,02%	3,74%
K	4,20%	4,50%	4,10%	4,60%	4,40%	4,80%	4,50%	5,00%	4,30%
Na	29,70%	29,41%	29,76%	29,41%	29,70%	29,43%	29,68%	29,29%	29,75%
SO4	63,00%	63,63%	63,11%	62,88%	61,68%	61,50%	61,33%	61,36%	61,95%
CO3	0,04%	0,02%	0,02%	0,03%	0,21%	0,43%	0,43%	0,33%	0,26%
Na2SO4	86,00%	86,32%	86,32%	85,15%	83,90%	82,98%	83,27%	82,45%	84,43%
Na2CO3	0,07%	0,03%	0,03%	0,05%	0,34%	0,69%	0,70%	0,53%	0,42%
NaCl	4,66%	3,69%	4,59%	4,65%	6,08%	5,78%	6,14%	6,02%	5,68%
K2SO4	8,77%	9,53%	8,58%	9,61%	8,97%	9,76%	9,11%	10,15%	8,80%
K2CO3	0,01%	0,00%	0,00%	0,01%	0,04%	0,09%	0,08%	0,07%	0,05%
KCl	0,49%	0,42%	0,47%	0,55%	0,68%	0,71%	0,70%	0,77%	0,62%

Table 27. Experimental data of recycled ash composition in Mill 1. Dry solids is the amount of diluted and suspended solids in the solution.

Experimental data	***Recycled ash (Product)(wt%)***								
Sample	1	2	3	4	5	6	7	8	9
Cl	0,40%	0,36%	0,41%	0,32%	0,38%	0,48%	0,57%	0,56%	0,61%
K	0,70%	0,70%	0,70%	0,60%	0,60%	0,90%	0,90%	1,00%	0,90%
Na	33,20%	33,20%	33,00%	32,99%	33,24%	33,18%	33,07%	32,93%	32,27%
SO4	68,17%	68,08%	68,09%	66,39%	68,29%	67,53%	66,25%	67,60%	67,01%
CO3	0,01%	0,00%	0,00%	0,00%	0,02%	0,08%	0,09%	0,08%	0,06%
Dry solids	89,90%	90,80%	89,30%	90,80%	91,20%	87,98%	88,90%	89,10%	88,25%

Table 28. Recycled ash composition calculated by the Recovery Boiler Design program developed by Metso Power. The experimental data of Cl, K and CO_3 are used, and the composition of Na and SO_4 are predicted by the program. Thereafter the program predicts the composition of different salts.

Calculated from RBD	***Recycled ash (Product)(wt%)***								
Sample	1	2	3	4	5	6	7	8	9
Cl	0,40%	0,36%	0,41%	0,32%	0,38%	0,48%	0,57%	0,56%	0,61%
K	0,70%	0,70%	0,70%	0,60%	0,60%	0,90%	0,90%	1,00%	0,90%
Na	31,91%	31,91%	31,91%	31,98%	31,99%	31,79%	31,80%	31,73%	31,80%
SO4	66,98%	67,03%	66,98%	67,10%	67,01%	66,75%	66,64%	66,63%	66,63%
CO3	0,01%	0,00%	0,00%	0,00%	0,02%	0,08%	0,09%	0,08%	0,06%
Na2SO4	97,77%	97,86%	97,77%	98,14%	98,01%	97,08%	96,92%	96,73%	96,91%
Na2CO3	0,02%	0,00%	0,00%	0,00%	0,03%	0,14%	0,16%	0,14%	0,10%
NaCl	0,65%	0,59%	0,67%	0,52%	0,62%	0,78%	0,92%	0,91%	0,99%
K2SO4	1,55%	1,55%	1,55%	1,33%	1,33%	1,98%	1,98%	2,20%	1,98%
K2CO3	0,00%	0,00%	0,00%	0,00%	0,00%	0,00%	0,00%	0,00%	0,00%
KCl	0,01%	0,01%	0,01%	0,01%	0,01%	0,02%	0,02%	0,02%	0,02%

Table 29. Experimental data of recycled ash composition in Mill 1. Dry solids is the amount of diluted and suspended solids in the solution.

Experimental data	***Reject (wt%)***								
Sample	1	2	3	4	5	6	7	8	9
Cl	4,82%	5,37%	7,45%	7,96%	7,04%	7,69%	9,47%	10,18%	7,85%
K	6,50%	6,30%	6,50%	6,50%	6,90%	6,40%	7,30%	7,40%	7,10%
Na	28,00%	28,70%	28,80%	28,80%	28,80%	28,70%	27,90%	28,70%	28,20%
SO4	60,78%	60,58%	58,41%	56,86%	58,25%	57,40%	54,72%	53,62%	56,43%
CO3	0,06%	0,05%	0,05%	0,07%	0,38%	0,89%	1,02%	0,86%	0,51%
Dry solids	31,76%	31,52%	31,52%	31,39%	31,49%	31,18%	30,76%	30,49%	31,11%

Table 30. Recycled ash composition calculated by the Recovery Boiler Design program developed by Metso Power. The experimental data of Cl, K and CO_3 are used, and the composition of Na and SO_4 are predicted by the program. Thereafter the program predicts the composition of different salts.

From RBD	*Reject (wt%)*								
Sample	1	2	3	4	5	6	7	8	9
Cl	4,82%	5,37%	7,45%	7,96%	7,04%	7,69%	9,47%	10,18%	7,85%
K	6,50%	6,30%	6,50%	6,50%	6,90%	6,40%	7,30%	7,40%	7,10%
Na	28,25%	28,45%	28,55%	28,61%	28,28%	28,81%	28,39%	28,37%	28,25%
SO4	60,37%	59,83%	57,45%	56,86%	57,40%	56,21%	53,82%	53,19%	56,29%
CO3	0,06%	0,05%	0,05%	0,07%	0,38%	0,89%	1,02%	0,86%	0,51%
Dry solids	31,76%	31,52%	31,52%	31,39%	31,49%	31,18%	30,76%	30,49%	31,11%
Na2SO4	78,63%	78,27%	74,92%	74,17%	74,23%	73,51%	69,13%	68,19%	72,52%
Na2CO3	0,09%	0,08%	0,08%	0,11%	0,59%	1,39%	1,57%	1,32%	0,78%
NaCl	7,00%	7,83%	10,83%	11,58%	10,15%	11,21%	13,56%	14,55%	11,27%
K2SO4	13,05%	12,50%	12,31%	12,15%	13,07%	11,78%	12,82%	12,83%	13,15%
K2CO3	0,02%	0,01%	0,01%	0,02%	0,11%	0,24%	0,31%	0,26%	0,15%
KCl	1,21%	1,30%	1,85%	1,97%	1,86%	1,87%	2,62%	2,85%	2,13%

Table 31. Process flows measured at the point of sampling for analysis.

Experimental data	*Process flows*								
Sample	1	2	3	4	5	6	7	8	9
Slurry flow (kg/h)	10736	13031	13114	13951	13523	12705	12296	14841	13619
Recirculation ratio (%)	16,4%	13,8%	13,5%	12,5%	11,5%	11,7%	12,1%	9,6%	10,5%

Mill 2

In this section the experimental data and corrected data by RBD for Mill 2 are presented. All data are taken at a temperature of 90ºC.

Table 32. Experimental data of ash composition at Mill 1.

Experimental data	*Ash composition (wt%)*				
Sample	1	2	3	4	5
Cl	4,2%	3,3%	3,1%	3,4%	4,4%
K	3,0%	3,5%	3,0%	2,9%	3,0%
Na	33,8%	34,4%	34,0%	34,7%	34,7%
SO4	43,2%	42,2%	42,8%	42,7%	40,5%
CO3	14,0%	18,5%	17,7%	17,2%	18,3%
Dry solids	98,9%	98,9%	98,9%	98,9%	98,9%

Table 33. Ash composition calculated by the Recovery Boiler Design program developed by Metso Power. The experimental data for Cl, K and CO_3 are used, and the composition of Na and SO_4 are predicted by the program. Thereafter the program predicts the composition of different salts.

Calculated from RBD	***Ash composition (wt%)***				
Sample	1	2	3	4	5
Cl	4,2%	3,3%	3,1%	3,4%	4,4%
K	3,0%	3,5%	3,0%	2,9%	3,0%
Na	33,4%	33,8%	34,0%	34,0%	34,3%
SO4	45,3%	40,9%	42,2%	42,5%	40,1%
CO3	14,0%	18,5%	17,7%	17,2%	18,3%
Na2SO4	63,7%	57,0%	59,3%	59,8%	56,4%
Na2CO3	23,5%	30,8%	29,7%	29,0%	30,7%
NaCl	6,6%	5,2%	4,9%	5,3%	6,9%
K2SO4	4,1%	4,2%	3,8%	3,7%	3,5%
K2CO3	1,6%	2,4%	2,0%	1,9%	2,0%
KCl	0,5%	0,4%	0,3%	0,3%	0,5%

Table 34. Experimental data of slurry composition. Dry solids is the amount of diluted and suspended solids in the solution.

Experimental data	***Slurry composition (wt%)***				
Sample	1	2	3	4	5
Cl, %	4,40%	3,19%	1,57%	2,63%	2,50%
K, %	3,50%	1,50%	1,49%	1,49%	1,93%
Na, %	33,95%	35,46%	34,86%	35,35%	36,70%
SO4, %	42,92%	42,94%	46,46%	45,72%	43,32%
CO3, %	14,36%	17,43%	16,69%	16,59%	18,11%
Dry solids %	40,03%	47,01%	44,24%	43,79%	45,01%

Table 35. Slurry composition calculated by the Recovery Boiler Design program developed by Metso Power. The experimental data for Cl, K and CO_3 are used, and the composition of Na and SO_4 are predicted by the program.

Calculated from RBD	***Slurry composition (wt%)***				
Sample	1	2	3	4	5
Cl	4,40%	3,19%	1,57%	2,63%	2,50%
K	3,50%	1,50%	1,49%	1,49%	1,93%
Na	33,14%	35,05%	34,72%	34,82%	34,79%
SO4	44,60%	42,83%	45,53%	44,47%	42,67%
CO3	14,36%	17,43%	16,69%	16,59%	18,11%
Na2SO4	62,09%	61,78%	65,66%	64,14%	61,10%
Na2CO3	23,88%	30,03%	28,75%	28,58%	30,98%
NaCl	6,83%	5,13%	2,52%	4,23%	3,99%
K2SO4	4,73%	1,91%	2,03%	1,98%	2,45%
K2CO3	1,93%	0,99%	0,95%	0,94%	1,32%
KCl	0,54%	0,16%	0,08%	0,14%	0,17%

Table 36. Experimental data of recycled ash composition in Mill 2. Dry solids is the amount of diluted and suspended solids in the solution.

Experimental data	***Recycled ash (Product)(wt%)***				
Sample	1	2	3	4	5
Cl	2,10%	1,20%	0,96%	2,35%	1,62%
K	1,00%	1,00%	1,00%	1,00%	0,94%
Na	36,48%	36,82%	34,96%	34,95%	36,06%
SO4	48,11%	47,22%	48,25%	47,22%	48,87%
CO3	14,87%	16,75%	16,16%	16,15%	17,10%
Dry solids	70,55%	70,20%	73,24%	63,81%	70,33%

Table 37. Recycled ash composition calculated by the Recovery Boiler Design program developed by Metso Power. The experimental data for Cl, K and CO_3 are used, and the composition of Na and SO_4 are predicted by the program. Thereafter the program predicts the composition of different salts.

Calculated from RBD	***Recycled ash (Product)(wt%)***				
Sample	1	2	3	4	5
Cl	2,10%	1,20%	0,96%	2,35%	1,62%
K	1,00%	1,00%	1,00%	1,00%	0,94%
Na	34,78%	35,04%	34,90%	35,06%	35,20%
SO4	47,25%	46,01%	46,98%	45,44%	45,14%
CO3	14,87%	16,75%	16,16%	16,15%	17,10%
Na2SO4	68,70%	66,90%	68,31%	66,08%	65,71%
Na2CO3	25,83%	29,10%	28,07%	28,05%	29,74%
NaCl	3,40%	1,95%	1,56%	3,81%	2,63%
K2SO4	1,42%	1,38%	1,41%	1,36%	1,27%
K2CO3	0,57%	0,64%	0,62%	0,61%	0,61%
KCl	0,07%	0,04%	0,03%	0,08%	0,05%

Table 38. Experimental data of recycled ash composition in Mill 1. Dry solids is the amount of diluted and suspended solids in the solution.

Experimental data	*Reject (wt%)*				
Sample	1	2	3	4	5
Cl	10,28%	7,31%	6,72%	5,95%	8,55%
K	6,47%	2,49%	5,98%	4,48%	6,93%
Na	31,37%	32,92%	34,42%	31,13%	33,64%
SO4	36,20%	37,26%	37,29%	36,22%	32,92%
CO3	13,02%	18,19%	18,34%	17,83%	18,56%
Dry solids	29,28%	30,08%	30,30%	30,32%	30,67%

Table 39. Recycled ash composition calculated by the Recovery Boiler Design program developed by Metso Power. The experimental data for Cl, K and CO_3 are used, and the composition of Na and SO_4 are predicted by the program. Thereafter the program predicts the composition of different salts.

Calculated from RBD	*Reject (wt%)*				
Sample	1	2	3	4	5
Cl	10,28%	7,31%	6,72%	5,95%	8,55%
K	6,47%	2,49%	5,98%	4,48%	6,93%
Na	31,42%	34,95%	32,40%	33,29%	31,96%
SO4	38,81%	37,06%	36,56%	38,45%	34,00%
CO3	13,02%	18,19%	18,34%	17,83%	18,56%
Na2SO4	51,19%	52,59%	48,77%	52,69%	44,59%
Na2CO3	20,51%	30,84%	29,22%	29,18%	29,08%
NaCl	15,12%	11,57%	9,99%	9,09%	12,50%
K2SO4	7,60%	2,70%	6,49%	5,11%	6,97%
K2CO3	3,24%	1,68%	4,14%	3,01%	4,83%
KCl	2,33%	0,62%	1,38%	0,92%	2,03%

Table 40. Process flows measured at the point of analysis.

Experimental data	*Process flows*				
Sample	1	2	3	4	5
Slurry (kg/h)	14093	14991	14994	15309	15498
Recirculation ratio (%)	27	10	10	40	25

Mill 3

Experimental data and data corrected by the program RBD are shown for the ESP ash, slurry, recycled solids and reject.

Table 41. Experimental composition of ingoing ash, slurry, recycled ash and reject in Mill 3. Dry solids are the amount of diluted and suspended solids in the solution.

Experimental data	***Ash***	***Slurry***	***Solids***	***Reject***
Cl	4,38%	6,70%	1,40%	12,80%
K	5,19%	7,20%	1,70%	13,00%
Na	33,80%	32,00%	34,80%	30,10%
SO4	31,40%	28,50%	33,00%	10,70%
CO3	26,10%	27,10%	23,40%	36,10%
Total weight, %	100,87%	101,50%	94,30%	102,70%
Dry solids, %	-	47,40%	82,40%	32,60%

Table 42. Composition of ingoing ash, slurry, recycled ash and reject calculated by the Recovery Boiler Design program developed by Metso Power. The experimental data for Cl, K and CO_3 are used, and the composition of Na and SO_4 are predicted by the program. Thereafter the program predicts the composition of different salts.

From RBD	***Ash***	***Slurry***	***Solids***	***Reject***
Cl	4,38%	6,70%	1,40%	12,80%
K	5,19%	7,20%	1,70%	13,00%
Na	34,21%	33,22%	35,86%	31,48%
SO4	30,12%	25,78%	37,64%	6,62%
CO3	26,10%	27,10%	23,40%	36,10%
Na2SO4	40,89%	33,81%	54,15%	7,87%
Na2CO3	42,32%	42,45%	40,21%	51,31%
NaCl	6,63%	9,80%	2,25%	16,98%
K2SO4	4,48%	5,29%	1,85%	2,34%
K2CO3	4,92%	7,06%	1,46%	16,24%
KCl	0,75%	1,59%	0,08%	5,26%

Table 43. Process flows measured at the point of analysis.

Experimental data **Sample**	***Process flows*** 1
Slurry (kg/h)	12985
Recirculation ratio (%)	50

Appendix D – Mass balances

Total balance

The total mass balance over the system can be seen below.

$\dot{m}_{ash\ in} + \dot{m}_{H_2O} - \dot{m}_{bleed} - \dot{m}_{rec.\ ash} = 0$
$\dot{m}_{ash\ in} \cdot x_{i,ash\ in} - \dot{m}_{bleed} \cdot x_{i,bleed} - \dot{m}_{rec.\ ash} \cdot x_{i,rec.ash} = 0$

Recirculation

When the reject flow and recirculation ratio are known, the recycled flow can be calculated.

$\dot{m}_{reject} = \dot{m}_{recirc.} + \dot{m}_{bleed}$
$\dot{m}_{recirc.} = \propto \cdot \dot{m}_{reject}$

Balance over centrifuge

The balance over the centrifuge gives the flow of the recycled ash, with a known recirculation ratio.

$\dot{m}_{slurry} = \dot{m}_{rec.ash} + \dot{m}_{bleed}$
$\dot{m}_{slurry} \cdot x_{i,slurry} = \dot{m}_{rec.ash} \cdot x_{i,rec.ash} + \dot{m}_{bleed} \cdot x_{i,bleed}$

Calculation procedure for ash and water flow

1. Amount suspended solids in slurry and recycled solids are calculated by using the dry solids content in slurry, solids and reject assuming that no suspended solids are present in the reject.

   $ss = DS - (100 - DS)(\frac{DS_{sat.sol.}}{100 - DS_{sat.sol.}})$

2. The flow recycled solids and reject flow can then be calculated:

   $\dot{m}_{rec.ash} = \dot{m}_{slurry} \frac{ss_{slurry}}{ss_{rec.ash}}$

   $\dot{m}_{reject} = \dot{m}_{slurry} - \dot{m}_{rec.ash}$

3. The recirculation ratio gives the recirculation and bleed flow:
   $\dot{m}_{recirc.} = \alpha\ \dot{m}_{reject}$

   $\dot{m}_{bleed} = \dot{m}_{reject} - \dot{m}_{recirc.}$

4. The ash and water flow can now be calculated by a mass balance over the leaching tank.
   $\dot{m}_{ash} = \dot{m}_{slurry} DS_{slurry} - \dot{m}_{recirc} DS_{sat.sol}$

   $\dot{m}_{H_2O} = \dot{m}_{slurry} - \dot{m}_{recirc} - \dot{m}_{ash}$

Appendix E – Excel data sheet, Model I

	A	B	C	D	E	F	G	H	I	J	K	L	M	N	O	P	Q	R
1	Mill:	Aracruz																
2	Project:																	
3	Date:				Susp solids in centr			85,20%			Efficiency							
4	Sign:				Susp solids in tank			35,46%			Cl-removal	84,4%						
5	Rev				Solubility			31,00%			K-removal	84,4%						
6	Case				Recirculation			14,06%			Na-recovery	79,8%						
7											SO4 recovery	79,9%						
8	Input data:										CO3-recovery	15,6%						
9																		
10	Ash	5498	kg/h			Tank						Centrifuge						
11	Water	4274	kg/h			Ash in	Water in	Recirc in	Slurry out	Solids	Liquid	Reject out	Bleed out	Recirc	Ash out	Balance	Efficiency	
12	T	90	°C		Flow (kg/h)	5498,10	4274,44	1150,70	10923,25	3873,15	7050,10	6081,81	5226,56	855,25	4545,99	0,00		
13	Susp solids in centr	85,20%			Cl	126,46	0,00	17,46	143,91	0,00	143,91	124,15	106,69	17,46	19,77	0,00	84,4%	
14	Solubility	31%			K	219,92	0,00	30,36	250,29	0,00	250,29	215,91	185,55	30,36	34,38	0,00	84,4%	
15	Recirculation	14,06%			Na	1649,43	0,00	54,63	1704,06	1253,76	450,29	388,45	333,82	54,63	1315,61	0,00	79,8%	
16					SO4	3436,32	0,00	112,78	3549,10	2619,39	929,71	802,02	689,24	112,78	2747,08	0,00	79,9%	
17	Ash analyses from RBD:				CO3	65,98	0,00	9,11	75,09	0,00	75,09	64,77	55,66	9,11	10,31	0,00	15,6%	
18					Water	0,00	4274,44	590,12	4864,57	0,00	4864,57	4196,45	3606,33	590,12	668,12	0,00		
19	Ash composition (comp)	wt%																
20	Cl	2,30%			% Cl	2,30%		1,52%	1,32%	0,00%	2,04%	2,04%	2,04%	2,04%	0,43%			
21	K	4,00%			%K	4,00%		2,64%	2,29%	0,00%	3,55%	3,55%	3,55%	3,55%	0,76%			
22	SO4	62,50%			%Na	30,00%		4,75%	15,60%	32,37%	6,39%	6,39%	6,39%	6,39%	28,94%			
23	Na	30,00%			%SO4	62,50%		9,80%	32,49%	67,63%	13,19%	13,19%	13,19%	13,19%	60,43%			
24	CO3	1,20%			%CO3	1,20%		0,79%	0,69%	0,00%	1,07%	1,07%	1,07%	1,07%	0,23%			
25	Tot	100,00%			%Water	0,00%	100,00%	51,28%	44,53%	0,00%	69,00%	69,00%	69,00%	69,00%	14,70%			
26						100,00%		70,78%	96,92%	100,00%	95,23%	95,23%	95,23%	95,23%	105,48%			
27																		
28					Dissolved in total				20,01%									
29					Dissolved in water				31,00%		26%	26%	26%	26%				
30	Molar mass	kg/kmol			%SS				35,46%						85,20%			
31	Na	22,9898			%DS				55,47%						85,30%			
32	SO4	96,0616																
33																		

Figure 38 The Excel calculation sheet is shown for Model I, with the predicted values for Ash 1 in Mill 1. The values marked red are required input data.

Appendix F – Predictions without recirculation

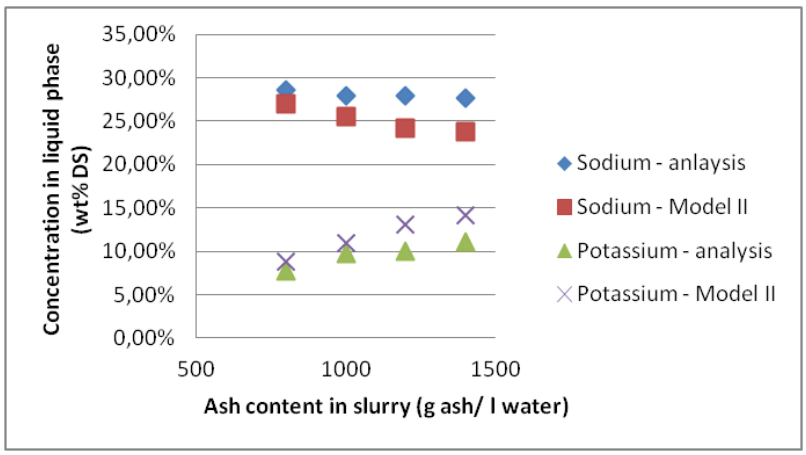

Figure 39.The composition in liquid phase (wt% DS) of Ash A depending on the ash content in slurry are shown in the figure. A comparison is done between the experimental data performed by Goncalves at 85ºC and the predicted values using Model II, with a dissolved ash amount in water of 31wt%.

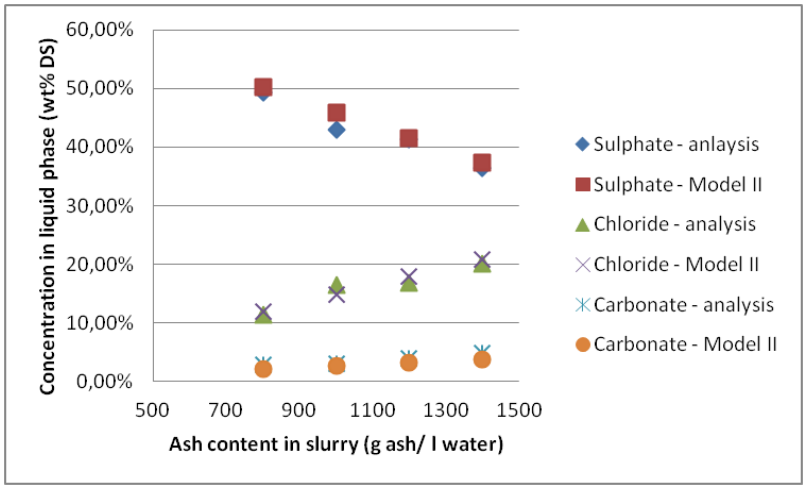

Figure 40.The composition in liquid phase (wt% DS) of Ash A depending on the ash content in slurry are shown in the figure. A comparison is done between the experimental data performed by Goncalves at 85ºC and the predicted values using Model II, with a dissolved ash amount in water of 31wt%.

Appendix G – Temperature dependence by Model II

Below the figures for Mill 2 predicted by Model II.

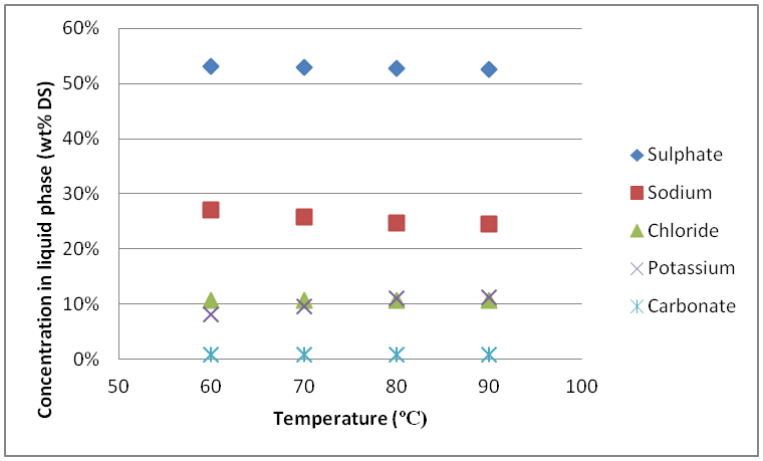

Figure 41. Temperature dependence predicted by Model II for Mill 2. A dissolved ash amount of 31 wt% is specified in the model.

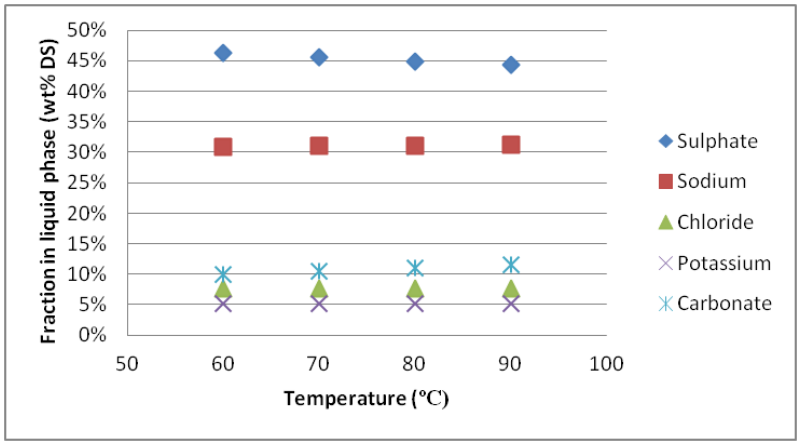

Figure 42. Temperature dependence predicted by Model II for Mill 2. A dissolved ash amount of 31 wt% is specified in the model.